


RESEARCH ARTICLE

Lotus japonicus karrikin receptors display divergent ligand-binding specificities and organ-dependent redundancy

Samy Carbonnel^{1,2}[✉], Salar Torabi^{1,2}[✉], Maximilian Griesmann¹[✉], Elias Bleek¹, Yuhong Tang³, Stefan Buchka¹, Veronica Basso¹[✉], Mitsuru Shindo⁴[✉], François-Didier Boyer⁵[✉], Trevor L. Wang⁶, Michael Udvardi³, Mark T. Waters^{7,8}, Caroline Gutjahr^{1,2}^{*}

1 LMU Munich, Faculty of Biology, Genetics, Biocenter Martinsried, Martinsried, Germany, **2** Technical University of Munich (TUM), TUM School of Life Sciences, Plant Genetics, Freising, Germany, **3** Noble Research Institute, Ardmore, Oklahoma, United States of America, **4** Institute for Materials Chemistry and Engineering, Kyushu University, Kasuga, Fukuoka, Japan, **5** Université Paris-Saclay, CNRS, Institut de Chimie des Substances Naturelles, Gif-sur-Yvette, France, **6** John Innes Centre, Norwich Research Park, Norwich, United Kingdom, **7** School of Molecular Sciences, The University of Western Australia, Perth, Australia, **8** Australian Research Council Centre of Excellence in Plant Energy Biology, The University of Western Australia, Perth, Australia

 These authors contributed equally to this work.

[✉] Current address: Department of Biology, University of Fribourg, Fribourg, Switzerland

* caroline.gutjahr@tum.de



 OPEN ACCESS

Citation: Carbonnel S, Torabi S, Griesmann M, Bleek E, Tang Y, Buchka S, et al. (2020) *Lotus japonicus* karrikin receptors display divergent ligand-binding specificities and organ-dependent redundancy. PLoS Genet 16(12): e1009249. <https://doi.org/10.1371/journal.pgen.1009249>

Editor: Hao Yu, National University of Singapore and Temasek Life Sciences Laboratory, SINGAPORE

Received: September 16, 2020

Accepted: November 3, 2020

Published: December 28, 2020

Copyright: © 2020 Carbonnel et al. This is an open access article distributed under the terms of the [Creative Commons Attribution License](https://creativecommons.org/licenses/by/4.0/), which permits unrestricted use, distribution, and reproduction in any medium, provided the original author and source are credited.

Data Availability Statement: Raw microarray data and CEL files are available at Gene Expression Omnibus (GEO) accession number GSE160075, <https://www.ncbi.nlm.nih.gov/geo/query/acc.cgi?acc=GSE160075>.

Funding: The study was supported by an Australian Research Council Future Fellowship (FT150100162) to MTW and initially by the SFB924 of the DFG to CG and subsequently by the Emmy Noether program of the DFG, grant GU1423/1-1 to

Abstract

Karrikins (KARs), smoke-derived butenolides, are perceived by the α/β -fold hydrolase KARRIKIN INSENSITIVE2 (KAI2) and thought to mimic endogenous, yet elusive plant hormones tentatively called KAI2-ligands (KLs). The sensitivity to different karrikin types as well as the number of *KAI2* paralogs varies among plant species, suggesting diversification and co-evolution of ligand-receptor relationships. We found that the genomes of legumes, comprising a number of important crops with protein-rich, nutritious seed, contain two or more *KAI2* copies. We uncover sub-functionalization of the two *KAI2* versions in the model legume *Lotus japonicus* and demonstrate differences in their ability to bind the synthetic ligand GR24^{ent-5DS} *in vitro* and in genetic assays with *Lotus japonicus* and the heterologous *Arabidopsis thaliana* background. These differences can be explained by the exchange of a widely conserved phenylalanine in the binding pocket of KAI2a with a tryptophan in KAI2b, which arose independently in KAI2 proteins of several unrelated angiosperms. Furthermore, two polymorphic residues in the binding pocket are conserved across a number of legumes and may contribute to ligand binding preferences. The diversification of KAI2 binding pockets suggests the occurrence of several different KLs acting in non-fire following plants, or an escape from possible antagonistic exogenous molecules. Unexpectedly, *L. japonicus* responds to diverse synthetic KAI2-ligands in an organ-specific manner. Hypocotyl growth responds to KAR₁, KAR₂ and *rac*-GR24, while root system development responds only to KAR₁. This differential responsiveness cannot be explained by receptor-ligand preferences alone, because *LjKAI2a* is sufficient for karrikin responses in the hypocotyl, while *LjKAI2a* and *LjKAI2b* operate redundantly in roots. Instead, it likely reflects differences between

CG. The funders had no role in study design, data collection and analysis, decision to publish, or preparation of the manuscript.

Competing interests: The authors have declared that no competing interests exist.

plant organs in their ability to transport or metabolise the synthetic KLs. Our findings provide new insights into the evolution and diversity of butenolide ligand-receptor relationships, and open novel research avenues into their ecological significance and the mechanisms controlling developmental responses to divergent KLs.

Author summary

Plant hormone signaling is crucial for development and for adequate responses to biotic and abiotic environmental conditions. The most recently discovered plant hormone receptor KARRIKIN INSENSITIVE 2 (KAI2), binds a small butenolide called karrikin that was discovered in smoke and induces germination of fire-following plants. Several lines of evidence suggest a yet elusive endogenous hormone, which acts as ligand for KAI2. Until its identification, synthetic karrikins or the strigolactone-like molecule GR24 are used to probe the karrikin signaling pathway. While the model plant *Arabidopsis* contains only one *KAI2* gene, several copies are maintained in other species suggesting sub-functionalization. We report that genomes of species in the legume hologalegina clade encode two *KAI2* versions. In *Lotus japonicus*, they diverge in their binding ability to synthetic ligands due to three amino acid changes in their binding pocket, of which two are conserved across legumes and one has independently occurred in several species across the angiosperm phylogeny. Surprisingly, *L. japonicus* hypocotyls react with developmental responses to two different karrikins (KAR₁, KAR₂) and a synthetic strigolactone *rac*-GR24, while root development responds only to KAR₁. This shows that there is not only diversity in ligand-receptor relationships but possibly also organ-specific uptake or metabolism of divergent butenolide molecules.

Introduction

Karrikins (KARs) are small butenolide compounds derived from smoke of burning vegetation that were identified as germination stimulants of fire-following plants [1]. They can also accelerate seed germination of species that do not grow in fire-prone environments such as *Arabidopsis thaliana*, which enabled the identification of genes encoding karrikin receptor components via forward and reverse genetics. The α/β -fold hydrolase KARRIKIN INSENSITIVE2 (KAI2) is thought to bind KARs, and interacts with the F-box protein MORE AXILLARY GROWTH 2 (MAX2) that is required for ubiquitylation of repressor proteins via the Skp1-Cullin-F-box (SCF) complex [2–9]. There are six known KARs, of which KAR₁ is most abundant in smoke-water and most active on seed germination of fire-following plants [1,10,11], but *Arabidopsis* responds more strongly to KAR₂, which lacks the methyl group at the butenolide ring that is characteristic for KAR₁ [2,3,11]. Both KAR₁ and KAR₂ are commercially available and commonly used in research.

Arabidopsis KAI2 regulates several traits in addition to seed germination, including light-dependent hypocotyl growth inhibition, cotyledon and rosette leaf area, cuticle thickness, root hair length and density, root skewing and lateral root density [4,12–15]. Moreover, the rice orthologs of *KAI2* (*D14-LIKE*) and *MAX2* (*D3*) are essential for root colonization by arbuscular mycorrhiza (AM) fungi, and are involved in regulating mesocotyl elongation [7,16,17]. These roles of KAI2, unrelated to smoke and seed germination, suggest that karrikins mimic yet-unknown endogenous (and possibly AM fungus-derived) signaling molecules that bind to

KAI2 to regulate plant development or AM symbiosis, and are provisionally called KAI2-ligands (KLs) [12,18].

Structurally, KARs resemble the apocarotenoid strigolactones (SLs), which were originally discovered in root exudates in the rhizosphere [19], where they act as germination cues for parasitic weeds [19] and as stimulants of AM fungi [20,21]. In addition to their function in the rhizosphere, SLs function endogenously as phytohormones and repress shoot branching [22,23]. SL signaling also affects secondary growth; and co-regulates lateral and adventitious root formation and rice mesocotyl elongation with the karrikin signaling pathway [7,15,24,25]. As with KARs, SLs are perceived by an α/β -fold hydrolase D14/DAD2 that, like KAI2, depends for function on a serine–histidine–aspartate catalytic triad within the ligand binding pocket [26,27]. As KAI2, D14 interacts with the SCF-complex via the same F-box protein MAX2 [9,26] to ubiquitylate repressors of the SMXL family and mark them for degradation by the 26S proteasome [28–31].

Phylogenetic analysis of the α/β -fold hydrolase receptors in extant land plants revealed that an ancestral KAI2 is already present in charophyte algae, while the so-called eu-KAI2 is ubiquitous among land plants. The strigolactone receptor gene, D14 evolved only in the seed plants likely through duplication of KAI2 and sub-functionalization [32]. An additional duplication in the seed plants gave rise to D14-LIKE2 (DLK2), an α/β -fold hydrolase of unknown function, which is transcriptionally induced in response to KAR treatment in a KAI2- and MAX2-dependent manner, and currently represents the best-characterized KAR marker gene in Arabidopsis [4,33]. Despite their similarity, KAI2 and D14 cannot replace each other in Arabidopsis, as shown by promoter swap experiments [34]. This indicates that their expression pattern does not determine their signaling specificity. Instead, this is reached by ligand-receptor preference, and most likely the tissue-specific presence of their ligands, as well as distinctive interaction with other proteins, such as repressors of the SMXL family to trigger downstream signaling [35].

In Arabidopsis and rice, in which KAR/KL signaling has so far been mostly studied, KAI2 is a single copy gene. However, KAI2 has multiplied and diversified in other species. For example, the *Physcomitrella patens* genome contains 11 genes encoding KAI2-like proteins [36]. Of these some preferentially bind KAR and others the SL 5-deoxystrigol *in vitro* and this preference is determined by polymorphic amino acids in a loop that determines the rigidity of the ligand-binding pocket [37]. The genomes of parasitic plants of the Orobanchaceae also contain several KAI2 copies. Some of these have evolved to perceive strigolactones, some can restore KAR-responses in Arabidopsis *kai2* mutants, and others do not mediate responses to any of these molecules in Arabidopsis [12,38,39]. Thus, in plant species with an expanded KAI2-family there is scope for a diverse range of ligands and ligand-binding specificities, as well as for diverse protein interaction partners. Apart from discriminating KARs from SLs, it was very recently reported that KAI2 genes have diversified in the genome of the fire follower *Brassica tournefortii* to encode KAI2 receptors, with different ligand preferences towards KAR₁ and KAR₂ [40]. Of these, *BtKAI2a* mediates stronger responses to KAR₂, while *BtKAI2b* mediates stronger responses to KAR₁, when expressed in the heterologous Arabidopsis background. This binding preference is determined by two valine (*BtKAI2a*) to leucine (*BtKAI2b*) substitutions at the ligand binding pocket [40]. Also, among plants with a single copy KAI2 gene, the responsiveness to karrikin molecules can differ significantly: Arabidopsis plants respond more strongly to KAR₂ than to KAR₁ [4,15]. In contrast, rice roots did not display any transcriptional response to KAR₂, not even for the marker gene *DLK2* [16]. It is yet unclear what determines these differences in KAR₂ responsiveness among plant species.

Legumes comprise a number of agronomically important crops and they are special among plants as most species in the family can form nitrogen-fixing root nodule symbiosis with

rhizobia in addition to arbuscular mycorrhiza. Given the possible diversity in KAI2-ligand specificities among plant species, we characterized the karrikin receptor machinery in a legume, using *L. japonicus* as a model. We found that KAI2 has duplicated prior to the diversification of legumes and that *L. japonicus* KAI2a and KAI2b differ in their binding preferences to synthetic ligands *in vitro* and in the heterologous Arabidopsis *kai2* and *kai2 d14* mutant backgrounds. We demonstrate that these ligand binding preferences can be explained by substitution of a highly conserved phenylalanine to a tryptophan in the binding pocket of LjKAI2b. This tryptophan occurs rarely also in other unrelated angiosperm species, and seems to have arisen several times independently. Two additional polymorphic residues that are conserved in the KAI2a and KAI2b clades across several legumes may also contribute to ligand binding preference. In addition, we found a surprising organ-specific responsiveness to synthetic KAI2-ligands, with *L. japonicus* hypocotyl development responding to KAR₁, KAR₂ and the strigolactone/karrikin analog *rac*-GR24, and root system development responding only to KAR₁. These responses depend only on LjKAI2a in hypocotyls, while LjKAI2a and LjKAI2b operate redundantly in roots. Together these findings suggest that a diversity of mechanisms may influence KAR/KL responses including receptor-ligand binding specificity or organ-specific interaction of KAI2 with other proteins.

Results

KAI2 underwent duplication prior to diversification of the legumes

To characterize the karrikin and the strigolactone perception machinery in *L. japonicus*, we retrieved KAI2, D14 and MAX2 by protein BLAST using Arabidopsis KAI2, D14 and MAX2 as templates. A phylogenetic tree revealed that *LjD14* (*Lj5g3v0310140.4*) is a single copy gene whereas *LjKAI2* has duplicated (Fig 1), resulting in two paralogs *LjKAI2a* (*Lj2g3v1931930.1*) and *LjKAI2b* (*Lj0g3v0117039.1*). The KAI2 duplication event must have occurred prior to the diversification of the legumes or at least before the separation of the Millettoids and the 'Hologalegina' clade [41] because a similar duplication pattern as in *L. japonicus* (Hologalegina) is also detected in pea, *Medicago truncatula* (both Hologalegina) and soybean (Millettoid). The Millettoid soybean genome additionally contains a third, more distantly related KAI2 copy (*KAI2c*).

The F-box protein-encoding gene *LjMAX2* also underwent duplication likely as a result of whole genome duplication, because the two *LjMAX2* copies are in two syntenic regions of the genome (S1A Fig). However, only one *LjMAX2* copy (*Lj3g3v2851180.1*) is functional. The other copy Ψ MAX2-like (*Lj0g3v0059909.1*) appears to be a pseudogene, as it contains an early stop codon, thus encoding a putative truncated protein of 216 instead of 710 amino acids (S1B Fig). It appears that an insertion of one nucleotide into Ψ MAX2-like created a frameshift, as manual deletion of thymine 453 restores a correct nucleotide and amino acid sequence (S1B Fig).

We hypothesized that *L. japonicus* (and other legumes) retained two intact KAI2 copies because they may have functionally diverged, perhaps through changes in their expression pattern and/or sequence, possibly resulting in a divergent spatial distribution, ligand affinity and/or ability to interact with other proteins. We examined transcript accumulation of *LjKAI2a* and *LjKAI2b*, as well as *LjD14* and *LjMAX2* in different organs of *L. japonicus* (S2 Fig). Overall, both *LjKAI2a* and *LjKAI2b* transcripts accumulated to higher levels than those of *LjD14* and *LjMAX2*. *LjKAI2a* transcripts accumulated approximately 100-fold more in aerial organs than *LjKAI2b*, whereas *LjKAI2b* accumulated 10-fold more than *LjKAI2a* in roots of adult plants, which were grown in a sand-vermiculite mix in pots under long day conditions (16h light /8h dark). However, 1-week-old seedlings grown on water-agar in Petri dishes under short-day

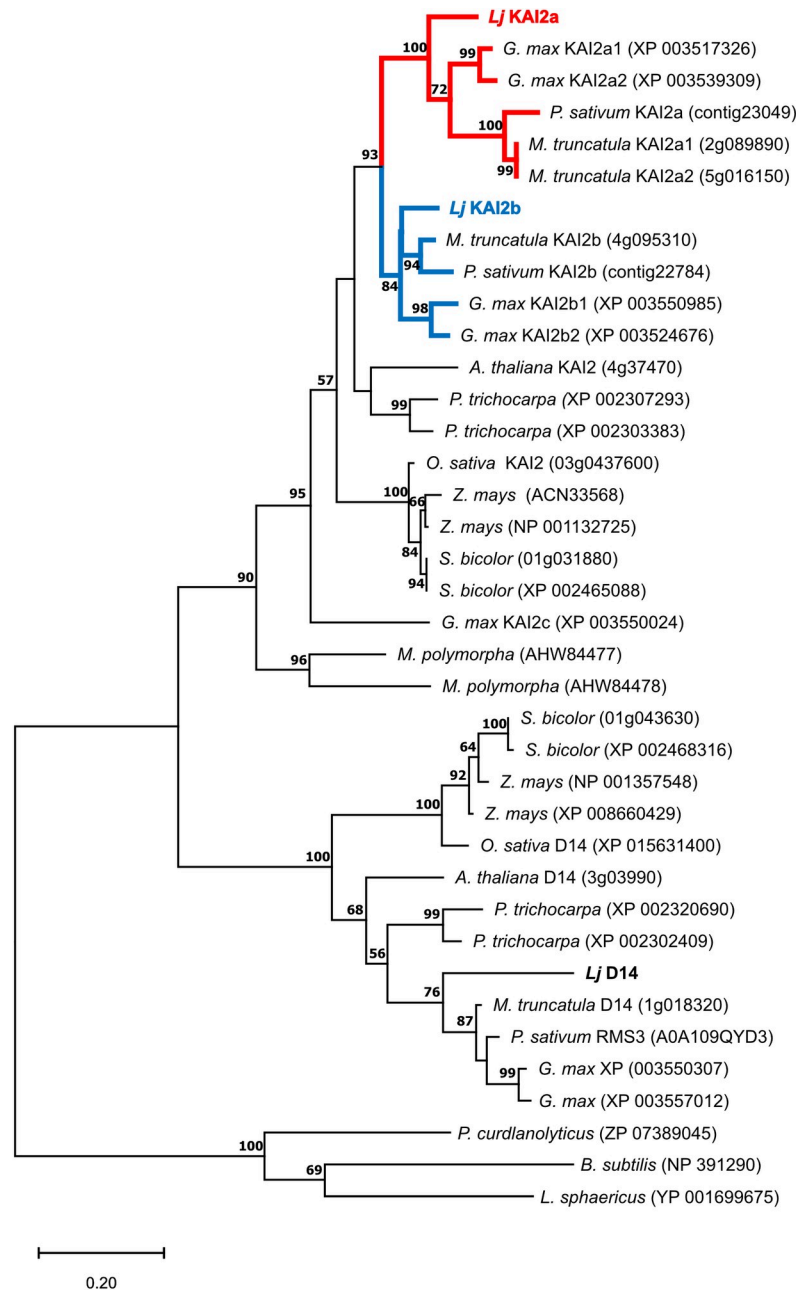


Fig 1. The KAI2 gene underwent duplication prior to diversification of the legumes. Phylogenetic tree of KAI2 and D14 rooted with bacterial RbsQ from indicated species (*Lotus japonicus*; *Glycine max*; *Pisum sativum*; *Medicago truncatula*; *Arabidopsis thaliana*; *Populus trichocarpa*; *Oryza sativa*; *Zea mays*; *Sorghum bicolor*; *Marchantia polymorpha*). MEGAX was used to align the protein sequences with MUSCLE and generate a tree inferred by Maximum Likelihood method [72]. The tree with the highest log likelihood (-7359.19) is shown. The percentage of trees in which the associated taxa clustered together is shown next to the branches. Values below 50 were ignored. KAI2 duplication in the legumes is highlighted by red and blue branches.

<https://doi.org/10.1371/journal.pgen.1009249.g001>

conditions (8h light/16h dark), displayed 10-fold higher transcript levels of *LjKAI2a* than *LjKAI2b* in both roots and hypocotyls (S2B Fig). Thus, *LjKAI2a* and *LjKAI2b* are regulated in an organ-specific, age- and/or environment-dependent manner, suggesting that their individual expression involves at least partially different transcriptional regulators.

Fusions of the four corresponding proteins with T-Sapphire or mOrange in transiently transformed *Nicotiana benthamiana* leaves showed similar subcellular localization as in Arabidopsis and rice [16,17,42,43]. T-Sapphire-MAX2 was detected exclusively in the nucleus, while the α/β -hydrolases (D14, KAI2a and KAI2b) fused to mOrange localized to the nucleus and cytoplasm (S3A Fig). Western blot analysis confirmed that the mOrange signal observed in the cytoplasm resulted from the full-length fusion protein and not from free mOrange (S3B Fig).

***L. japonicus* KAI2a, KAI2b and D14 can replace their orthologs in Arabidopsis**

To examine whether both *Lj*KAI2a and *Lj*KAI2b function in a canonical manner, we employed a well-established hypocotyl elongation assay in Arabidopsis [12,34], after transgenically complementing the *Arabidopsis thaliana* *kai2-2* mutant [4] with *Lj*KAI2a and *Lj*KAI2b driven by the *At*KAI2 promoter. Both restored inhibition of hypocotyl elongation in the *kai2-2* mutant (Fig 2A and 2B). *Lj*D14 driven by the *At*KAI2 promoter was unable to restore hypocotyl growth inhibition, but it restored repression of shoot branching of the Arabidopsis *d14-1* mutant [4], when driven by the Arabidopsis *D14* promoter. As expected, *Lj*KAI2a and *Lj*KAI2b could not do the same (Fig 2C and 2D). Together with the phylogenetic analysis (Fig 1), these results demonstrate that *L. japonicus* KAI2a and KAI2b are both functional orthologs of the Arabidopsis karrikin/KL receptor gene KAI2, whereas *L. japonicus* D14 is the functional orthologue of the Arabidopsis strigolactone receptor gene D14. Furthermore, the *L. japonicus* KAI2 genes are not interchangeable with D14 [34].

***Lotus japonicus* KAI2a and KAI2b differ in their ligand binding specificity**

To explore whether *L. japonicus* KAI2a and KAI2b can mediate hypocotyl responses to karrikins, we quantified hypocotyl length of the *Atkai2-2* lines transgenically complemented with *Lj*KAI2a or *Lj*KAI2b after treatment with KAR₁ and KAR₂ (Fig 3A and 3B). Two independent lines complemented with *Lj*KAI2a displayed a similar reduction in hypocotyl growth in response to both KAR₁ and KAR₂. However, the two lines expressing *Lj*KAI2b responded more strongly to KAR₁ than to KAR₂, contrasting with the common observation, that Arabidopsis hypocotyl growth tends to be more responsive to KAR₂ [4,44]. We wondered if the preference towards a specific KAR compound is also observed with KAI2 from other species. To this end, we tested the karrikin response in a line resulting from a cross of the *kai2* mutant *htl-2* with an Arabidopsis line transgenic for the cDNA of the rice *D14L/KAI2* [16]. In contrast to *Lj*KAI2b, *OsD14L/KAI2* mediated a stronger response to KAR₂ than to KAR₁ (Fig 3C). Thus, the differential responsiveness of transgenic Arabidopsis lines to KAR₁ and KAR₂ does not result from a general incompatibility of a heterologous KAI2 protein with the Arabidopsis background, but suggests different ligand affinities of the transgenic receptors to the karrikins or their possible metabolised products [34,40].

The two enantiomers of the synthetic strigolactone *rac*-GR24, namely GR24^{5DS} and GR24^{ent-5DS}, trigger developmental and transcriptional responses via D14 as well as KAI2, respectively, in Arabidopsis [15,45]. For some KAI2-mediated responses, GR24^{ent-5DS} was shown to be more active than karrikin [46] and it has been hypothesized that karrikin may need to be metabolized *in planta*, to yield a high affinity KAI2 ligand, while this may not be necessary for GR24^{ent-5DS} [34,46,47]. We examined whether *Lj*KAI2a and *Lj*KAI2b can mediate hypocotyl growth responses to GR24^{5DS} and GR24^{ent-5DS} in the *Arabidopsis thaliana* *d14-1 kai2-2* double mutant background (Fig 3D). Lines expressing *Lj*KAI2a responded to both enantiomers with reduced hypocotyl elongation, but displayed a much stronger response to the preferred KAI2 ligand GR24^{ent-5DS}. Unexpectedly, the lines expressing *Lj*KAI2b did not

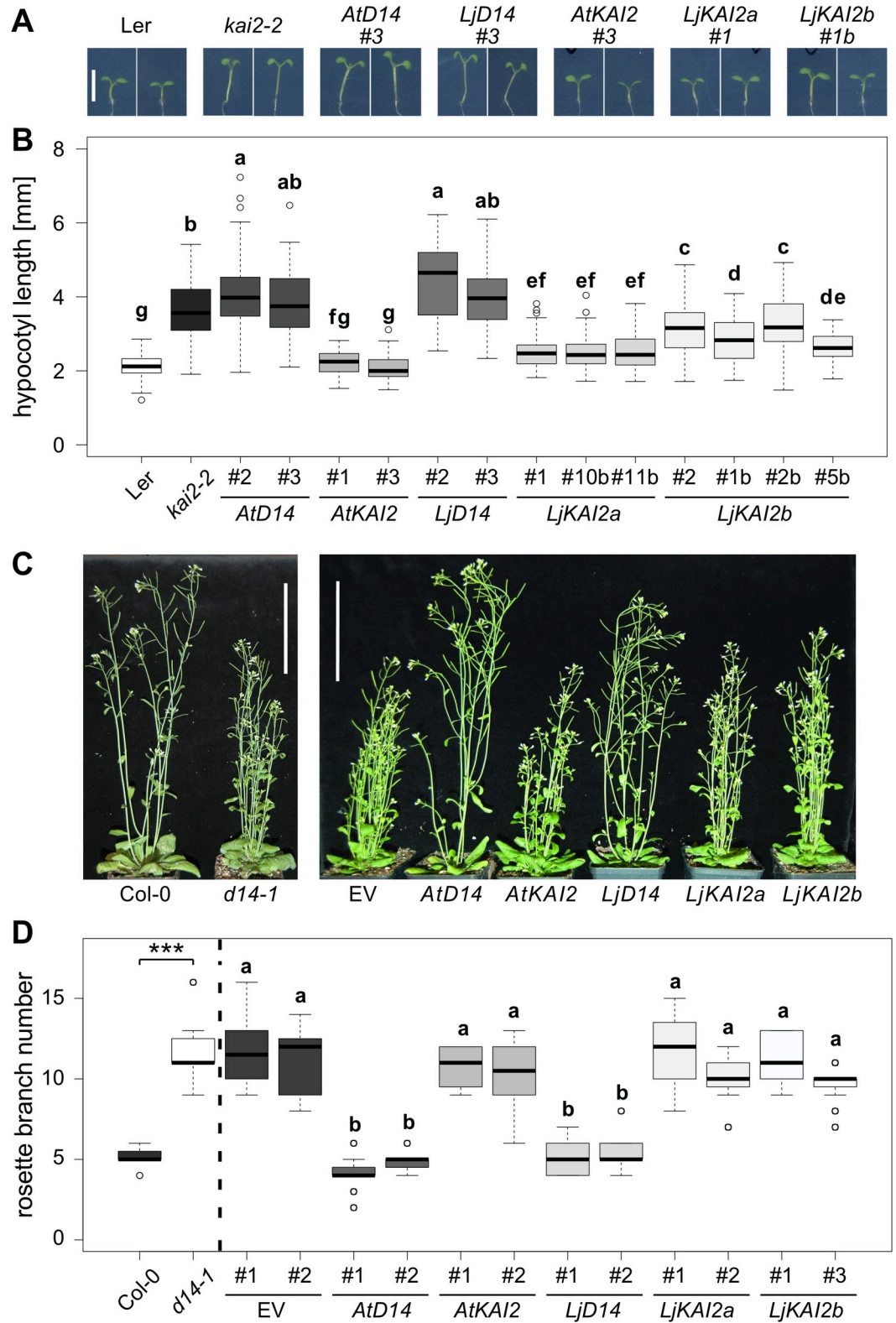


Fig 2. *Lotus japonicus* D14, KAI2a and KAI2b can replace D14 and KAI2 in Arabidopsis, respectively. (A-B) Hypocotyl length of *A. thaliana* wild-type (*Ler*), *kai2-2* and *kai2-2* lines complemented by *AtD14*, *AtKAI2*, *LjD14*, *LjKAI2a* and *LjKAI2b*, driven by the *AtKAI2* promoter at 6 days post germination (dpg). Seedlings were grown in 16h light/8h dark periods (n = 37–122). Scale bar = 5mm. (C) Shoots of *A. thaliana* Col-0 and *d14-1*, *d14-1*, with an empty vector (EV) or *LjKAI2a* and *LjKAI2b*.

complemented with *AtD14*, *AtKAI2*, *LjD14*, *LjKAI2a* and *LjKAI2b*, driven by the *AtD14* promoter at 26 dpv. Scale bar = 10 cm. (C) Rosette branch number at 26 dpv of *A. thaliana* wild-type (Col-0), *d14-1* and *d14-1* lines carrying an empty vector (EV) or plasmids containing *AtD14*, *AtKAI2*, *LjD14*, *LjKAI2a* and *LjKAI2b*, driven by the *AtD14* promoter (n = 24). Letters indicate different statistical groups (ANOVA, post-hoc Tukey test).

<https://doi.org/10.1371/journal.pgen.1009249.g002>

significantly respond to either of the two enantiomers. This contrasting sensitivity to GR24 enantiomers together with the differences in response to KAR₁ and KAR₂ suggests that *LjKAI2a* and *LjKAI2b* differ in their binding pocket, resulting in divergent affinity to the synthetic ligands.

Replacement of a conserved phenylalanine by a tryptophan at the binding pocket of KAI2b explains rejection of GR24^{ent-5DS}

We used differential scanning fluorimetry (DSF) to examine whether purified recombinant *LjKAI2a* and *LjKAI2b* (S4A Fig) display a different ligand affinity *in vitro*, employing GR24^{5DS} and GR24^{ent-5DS} as model ligands (Figs 4 and S4). The DSF assay has been widely used for deducing GR24^{5DS} and GR24^{ent-5DS} binding to D14 and KAI2 proteins respectively, by means of thermal destabilization [26,34,40,48–50]. However, DSF is unfortunately not suitable for the characterization of karrikin binding [34,40]. Neither *LjKAI2a* nor *LjKAI2b* were destabilized in the presence of GR24^{5DS} (S4B Fig). GR24^{ent-5DS} induced a significant thermal destabilization of *LjKAI2a* at a concentration > 50 μM (Fig 4C). In contrast, it did not cause any significant thermal shift of *LjKAI2b* (Fig 4D), thus recapitulating the difference in hypocotyl growth response between Arabidopsis lines expressing *LjKAI2a* and *LjKAI2b* (Fig 3D).

We found 16 conserved amino acid differences between the KAI2a and the KAI2b clade of the investigated legumes (S5 Fig), which may contribute to functional diversification of KAI2a and KAI2b. Modelling of *LjKAI2a* and *LjKAI2b* on the KAR₁-bound *AtKAI2* crystal structure (4JYM) [5] revealed that only three of these were located at the binding pocket, namely L160/M161, S190/L191 and M218/L219 (for the KAI2a/KAI2b comparison, Fig 4A and 4B). Out of these three, L219 was conserved between *LjKAI2b* and the KAI2 proteins from Arabidopsis and rice, which displayed an opposite response pattern to KAR₁ and KAR₂ compared to *LjKAI2b*, when expressed in the Arabidopsis background (Fig 3). Therefore, we concluded that the M218/L219 polymorphism likely does not play a major role in determining the observed differential ligand-preference between *LjKAI2a* and *LjKAI2b* and discounted it as a candidate. However, we also found that in *LjKAI2b* exclusively, a highly conserved phenylalanine inside the pocket is replaced by tryptophan at position 158 (S5 Fig). Although this tryptophan is not conserved among other legume KAI2b versions used for the alignment (S5 Fig), we predicted that this bulky residue should have a strong impact on ligand binding.

To understand the impact of the three divergent candidate amino acids on ligand binding, we generated chimeric receptor proteins (S4A Fig). Exchanging only the two amino acids that are conserved across KAI2a and KAI2b clades comprising the investigated legumes (S5 Fig) was sufficient to influence the melting temperature of the two proteins in response to GR24^{ent-5DS}. *LjKAI2a*^{M160,L190} became less responsive relative to *LjKAI2a* and displayed a slight shift in melting temperature only with 200 μM GR24^{ent-5DS} (Fig 4E), whereas *LjKAI2b*^{L161,S191} gained a weak ability to respond to GR24^{ent-5DS} at 200 μM (Fig 4F). When all three amino acids were swapped, the melting response to GR24^{ent-5DS} was entirely switched between the two receptor proteins: *LjKAI2a*^{M160,L190,W157} did not display any thermal shift in presence of GR24^{ent-5DS} (Fig 4G), whereas *LjKAI2b*^{L161,S191,F158} gained a strong response to GR24^{ent-5DS} and displayed a thermal shift with ligand concentrations as low as 25 μM (Fig 4H). Thus, *LjKAI2b*^{L161,S191,F158} seemed to be slightly more prone to ligand-induced destabilisation

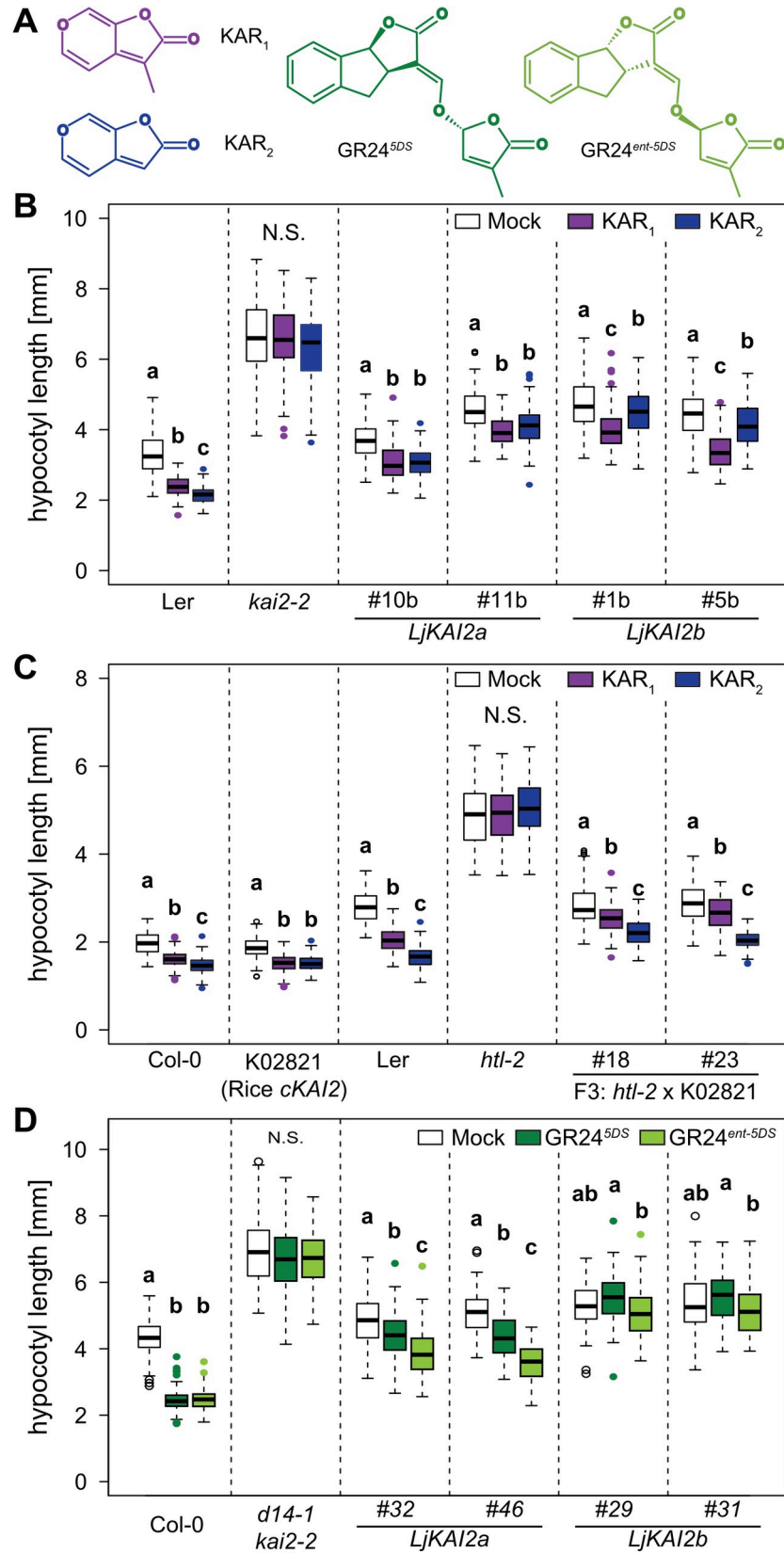


Fig 3. *Lotus japonicus* KAI2a, KAI2b and rice D14L confer divergent hypocotyl growth responses to KAR₁ and KAR₂ in Arabidopsis. (A) Structures of KAR₁, KAR₂, GR24^{5DS} and GR24^{ent-5DS}. (B-C) Hypocotyl length of *A. thaliana kai2* mutants complemented with KAI2 from *A. thaliana*, *L. japonicus* and rice, after treatment with solvent (Mock), 1 μM KAR₁ or KAR₂ at 6 dpg. (B) *Ler* wild-type, *kai2-2* and *kai2-2* lines complemented with *AtKAI2*, *LjKAI2a* and *LjKAI2b*, driven by the *AtKAI2* promoter (n = 33–128). (C) *Ler* and Col-0 wild-type, *htl-2* (*Ler*), K02821-line transgenic for *p35S:OsD14L* (Col-0), and two homozygous F₃ lines from the *htl-2* x K02821 cross [16] (n = 80–138). (D) Hypocotyl length of *A. thaliana* Col-0 wild-type, *d14-1 kai2-2* double mutants, and *d14-1 kai2-2* lines complemented with *LjKAI2a* and *LjKAI2b*, driven by the *AtKAI2* promoter after treatment with solvent (Mock), 1 μM GR24^{5DS} or GR24^{ent-5DS} (n = 59–134). (B-D) Seedlings were grown in 8h light/16h dark periods. Letters indicate different statistical groups (ANOVA, post-hoc Tukey test).

<https://doi.org/10.1371/journal.pgen.1009249.g003>

than wild-type *LjKAI2a*. As W158 appeared to be a critical amino acid for restricting the response to GR24^{ent-5DS}, we also tested whether swapping F157 with W158 alone would suffice to exchange the ability of the receptors to respond to GR24^{ent-5DS}. In effect, *LjKAI2b*^{F158} recapitulated the response of *LjKAI2a* to GR24^{ent-5DS} and likewise *LjKAI2a*^{W157} resembled *LjKAI2b* (Fig 4I and 4J). Thus, changing this one amino acid in the binding pocket was sufficient to swap ligand specificity. We conclude that the F158/W159 polymorphism predominantly determines the ability of *LjKAI2* proteins to bind GR24^{ent-5DS}, while there is a weaker contribution of L160/M161 and S190/L191.

As an alternative means to probe ligand-receptor interactions, intrinsic tryptophan fluorescence assays confirmed the response of wild-type *LjKAI2a* and *LjKAI2b* and all mutant versions to GR24^{ent-5DS} (S6 Fig). Unfortunately, because GR24^{ent-5DS} precipitated above 500 μM, this assay did not allow us to calculate K_d values because saturation of the response could not be achieved. Nevertheless, the qualitative results reiterate the strong impact of F158/W159 on the relative affinities of *LjKAI2a* and *LjKAI2b* for GR24^{ent-5DS}.

To examine whether the three amino acid residues determine ligand discrimination *in planta*, we transformed Arabidopsis *d14 kai2* double mutants with the mutated *LjKAI2a* and *LjKAI2b* genes driven by the Arabidopsis *KAI2* promoter and performed the hypocotyl growth assay in the presence of GR24^{ent-5DS}. Swapping only the two amino acids conserved in legumes (M160/L161 and S190/L191) was insufficient to exchange the GR24^{ent-5DS} response between lines expressing *LjKAI2a* vs. *LjKAI2b*. However, swapping all three amino acids, negatively affected the capacity of *LjKAI2a*^{M160,L190,W157} to mediate a hypocotyl response to GR24^{ent-5DS}, whereas it reconstituted a response via *LjKAI2b*^{L161,S191,F158} in three independent transgenic lines (Fig 5A and 5B). Although these results do not rule out a contribution of M160/L161 and S190/L191 towards ligand preference, they confirm that the phenylalanine to tryptophan substitution at position 157/158 is critical for determining the difference in GR24^{ent-5DS} binding preference between the two *L. japonicus* karrikin receptors KAI2a and KAI2b.

The phenylalanine to tryptophan exchange occurred in other angiosperms independently

The phenylalanine-to-tryptophan transition requires two base changes at position two and three of the codon. We asked whether this change also occurred in other species and searched for KAI2 sequences across the plant phylogeny by BLAST-P against the EnsemblPlants, NCBI and 1KP databases [51], and retrieved KAI2 sequences of the parasitic plants *Striga hermonthica*, *Orobancha fasciculata* and *Orobancha minor* from Conn et al. 2015 [38]. This analysis showed that the *KAI2c* copy, we detected in the soybean genome (Fig 1) occurred in all analysed genomes of Millettoid legumes, the Genistoid legume *Lupinus albus* and the Mimoid legume *Prosopis alba* (S7 Fig). This suggests that the members of the Hologalegina clade, such as *L. japonicus*, have secondarily lost *KAI2c*. Importantly, among the 156 KAI2 sequences we analysed, ten in addition to *LjKAI2b* contain a tryptophan at the position corresponding to

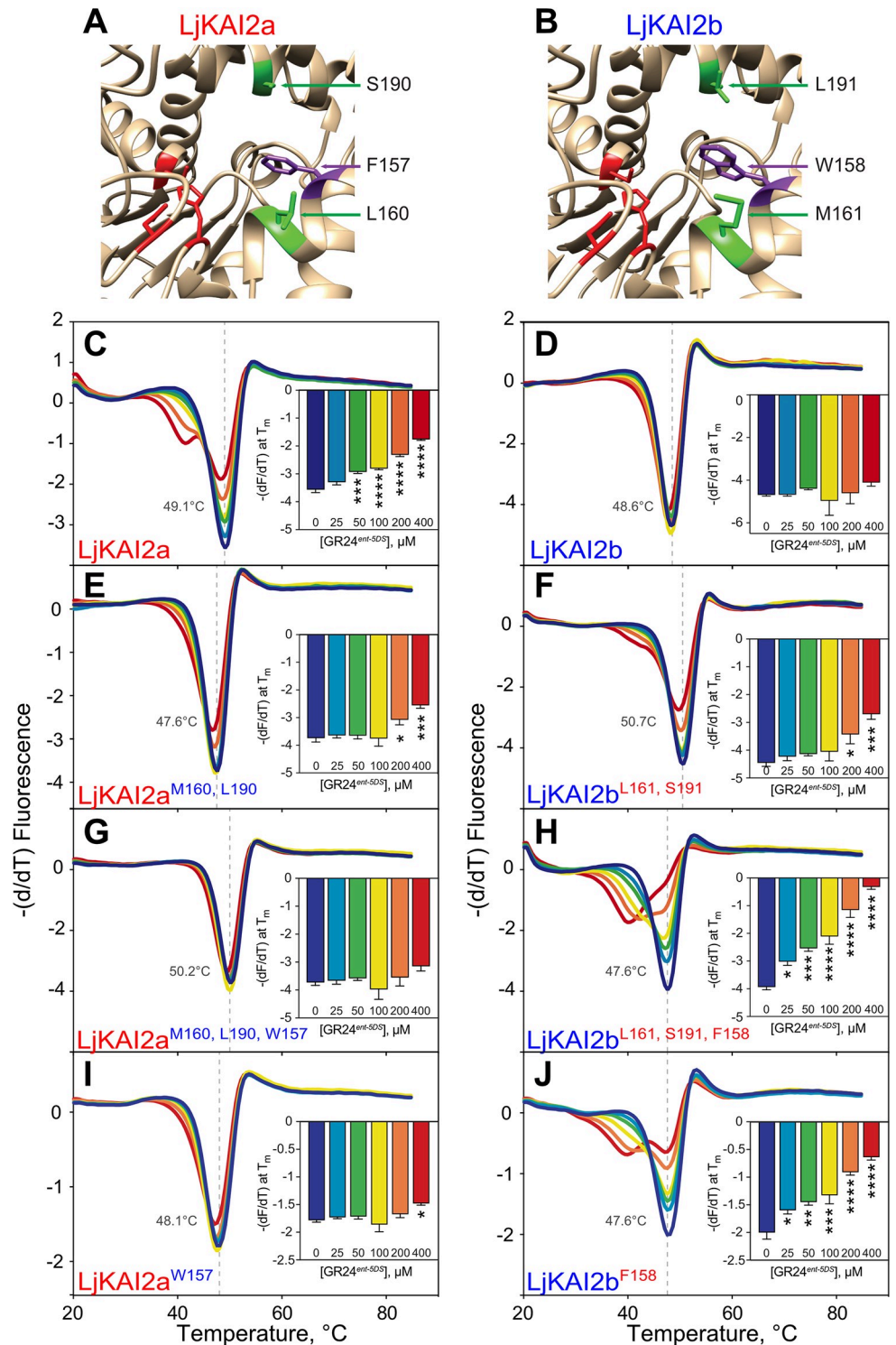


Fig 4. Binding of GR24^{ent-SDS} to LjKAI2a is determined by three amino acids. (A-B) The ligand-binding cavity regions of LjKAI2a and LjKAI2b proteins after structural homology modelling on the KAI2 crystal structure of *A. thaliana* [5]. Conserved residues in the cavity that differ between the KAI2a and KAI2b clades, and that are also different between LjKAI2b and AtKAI2, are shown in green. The phenylalanine residue in LjKAI2a, which is changed to tryptophan in LjKAI2b, is shown in violet. The catalytic triad is coloured in red. (C-J) DSF curves of purified SUMO fusion proteins of (C-D) wild-type LjKAI2a and LjKAI2b, and (E-J) versions with swapped amino acids (E-F) LjKAI2a^{M160,L190}, LjKAI2b^{L161,S191}, (G-H) LjKAI2a^{W157,M160,L190}, LjKAI2b^{F158,L161,S191}, (I-J) LjKAI2a^{W157},

LjKAI2b^{F158} at the indicated concentrations of GR24^{ent-5DS}. The first derivative of the change of fluorescence was plotted against the temperature. Each curve is the arithmetic mean of three sets of reactions, each comprising four technical replicates. Peaks indicate the protein melting temperature. The shift of the peak in *LjKAI2a* indicates ligand-induced thermal destabilisation consistent with a protein-ligand interaction. Insets plot the minimum value of (-dF/dT) at the melting point of the protein as determined in the absence of ligand (means ± SE, n = 3). Asterisks indicate significant differences to the solvent control (ANOVA, post-hoc Dunnett test, N.S.>0.05, *≤0.05, **≤0.01, ***≤0.001, ****≤0.0001).

<https://doi.org/10.1371/journal.pgen.1009249.g004>

157 in *Arabidopsis* KAI2 (S7 Fig). One of them was present in another legume (*Prosopis alba*). Five were present in other eudicots, of which three were in the Lamiales (Paulowniaceae: *Paulownia fargesii*; Phrymaceae: *Erythranthe guttata*, Orobanchaceae: *Orobanche fasciculata*) and two in the Ericales (Primulaceae: *Ardisia evoluta* and *Ardisia humilis*). Furthermore, we found four in monocots of the Bromeliaceae (*Ananas comosus*), Dioscoreaceae (*Dioscorea rotundata*) and Iridaceae (*Sisyrinchium angustifolium*). In these species, W157 does not co-occur with M160 and L190 as in *LjKAI2b*, but mostly in combination with the more widely conserved

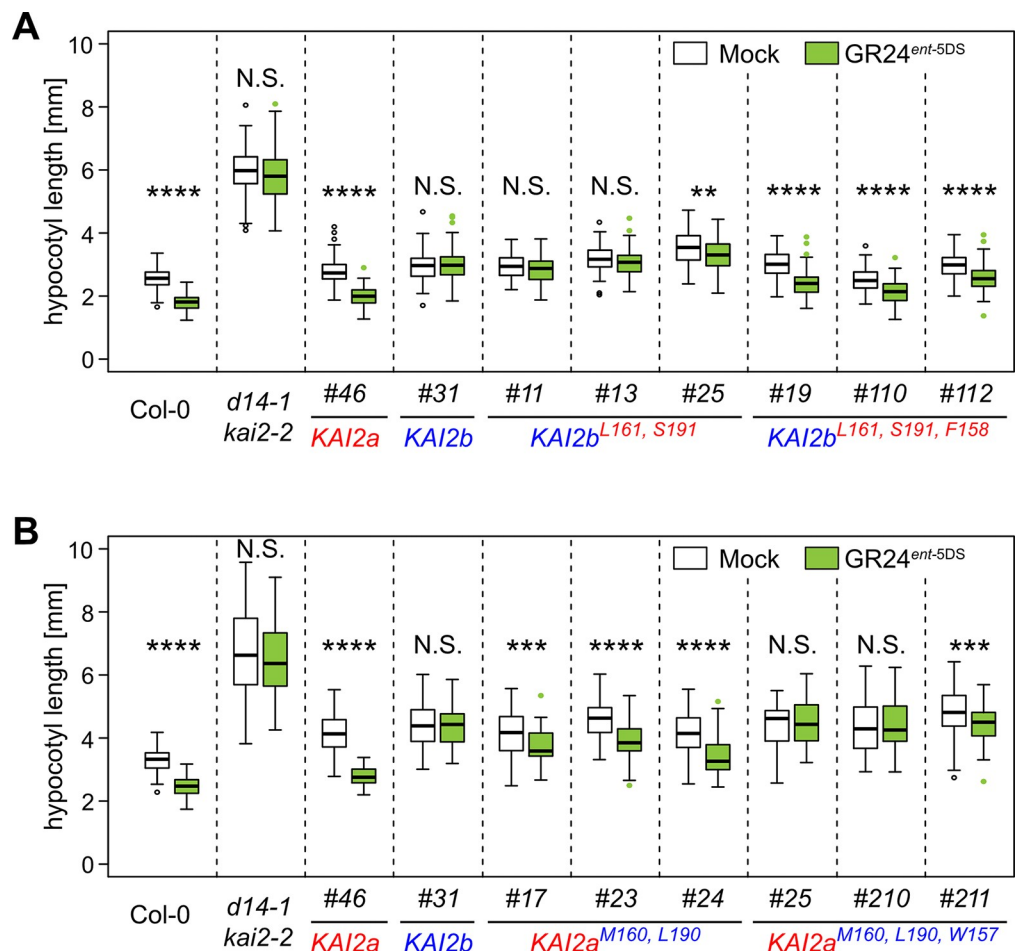


Fig 5. Amino acid swaps reverse sensitivity of *LjKAI2a* and *LjKAI2b* to GR24^{ent-5DS} in *Arabidopsis* hypocotyls. Hypocotyl length of *A. thaliana* Col-0 wild-type, *d14-1 kai2-2* double mutants, and *d14-1 kai2-2* lines complemented with *LjKAI2a* and *LjKAI2b* variants driven by the *AtKAI2* promoter and after treatment with solvent (Mock), 1 μ M GR24^{5DS} or GR24^{ent-5DS}. (A) *LjKAI2a*^{M160, L190} and *LjKAI2a*^{M160, L190, W157} (n = 46–84). (B) *LjKAI2b*^{L161, S191} and *LjKAI2b*^{L161, S191, F158} (n = 49–102). (A–B) Seedlings were grown in 8h light/16h dark periods Asterisks indicate significant differences versus mock treatment (Welch t.test, *≤0.05, **≤0.01, ***≤0.001, ****≤0.0001).

<https://doi.org/10.1371/journal.pgen.1009249.g005>

residues L160 and A190 and also with L160 and L190 in *Prosopis alba* and *Ananas comosus* (S7 Fig). The genomes of all dicotyledon species encoding a KAI2 version with W157 contained at least one second copy encoding F157. In the monocot *Dioscorea rotundata* two KAI2 copies encoded the W157, whereas in *Ananas comosus* and *Sisyrinchium angustifolium*, we detected only one KAI2 copy. However, we cannot exclude the existence of additional copies as several transcriptomes in the 1KP database are likely incomplete.

In summary, we demonstrate that the F to W transition has occurred several times independently in the angiosperms without co-dependency on M160 and L190 of LjKAI2b, and in most cases it occurred in a duplicate KAI2 version. Thus, the binding pocket of KAI2 proteins appears to be subject to diversification, broadening the range of diverse KAI2-ligand variants that can be recognized, and at the same time extending the opportunities for binding- and signaling-specificity through KAI2 variants with a less (F157) and/or more (W157) restrictive binding-pocket.

Characterization of *L. japonicus* karrikin and strigolactone receptor mutants

To explore the roles of LjKAI2a and LjKAI2b in *L. japonicus*, we characterized mutants in these genes as well as D14 and MAX2. We identified LORE1 retrotransposon insertions in *L. japonicus* KAI2a, KAI2b and MAX2 (*kai2a-1*, *kai2b-3*, *max2-1*, *max2-2*, *max2-3*, *max2-4*) in available collections [52,53] and nonsense mutations in D14 and KAI2b (*d14-1*, *kai2b-1*, *kai2b-2*) by TILLING [54] (Fig 6A, S1 Table). Since some of the *max2* and *kai2b* mutants were impaired in seed germination or production (S1 Table) we continued working with *kai2b-1*, *kai2b-3*, *max2-3* and *max2-4*. Quantitative RT-PCR analysis revealed that all mutations caused reduced transcript accumulation of the mutated genes in roots of the mutants except for *d14-1* (S8 Fig). Furthermore, the transcript accumulation of LjKAI2a and LjKAI2b was not affected by mutation of the respective other paralog (S8A Fig).

The LORE1 insertion in the *kai2a-1* mutant is located close (19 bp) to a splice acceptor site. Since some LjKAI2a transcript accumulated in the mutant, we sequenced this residual transcript to examine the possibility that a functional protein could still be made through loss of LORE1 by splicing. We found that indeed a transcript from ATG to stop accumulates in *kai2a-1* but it suffers from mis-splicing leading to a loss of the LORE1 transposon plus 15 bp (from 369–383), corresponding to five amino acids (YLNDV) at position 124–128 of the protein (S9A and S9B Fig). This amino-acid stretch reaches from a loop at the surface of the protein into the cavity of the binding pocket (S9C Fig). The artificial splice variant did not rescue the Arabidopsis *kai2-2* hypocotyl phenotype, confirming that it is not functional *in planta* and showing that the amino acids 124-YLNDV-128 are essential for LjKAI2a function (S9D Fig).

Karrikin and *rac*-GR24 cause reduction in hypocotyl growth of *L. japonicus* in an LjKAI2a-dependent manner

The *d14-1* and all *max2* mutants displayed increased shoot branching, indicating that the *L. japonicus* strigolactone receptor components D14 and MAX2 are involved in shoot branching inhibition (Fig 6B and 6C), as for Arabidopsis, pea and rice [4,43,55,56]. In addition, *d14* and *max2* mutants had smaller leaves (Fig 6D), a phenotype that has not yet been associated with strigolactone signaling in other dicotyledon species. Surprisingly, *kai2a* and *kai2b* single mutants as well as *kai2a-1 kai2b-1* double mutants or *max2* mutants did not display the canonical elongated hypocotyl phenotype, which is observed in Arabidopsis [4] also in white light conditions (Figs 2, 3 and 5). If anything, the *kai2a-1 kai2b-1* and *max2* mutant hypocotyls were shorter than those of the wild type (Fig 6E). This indicates that the requirement of KL

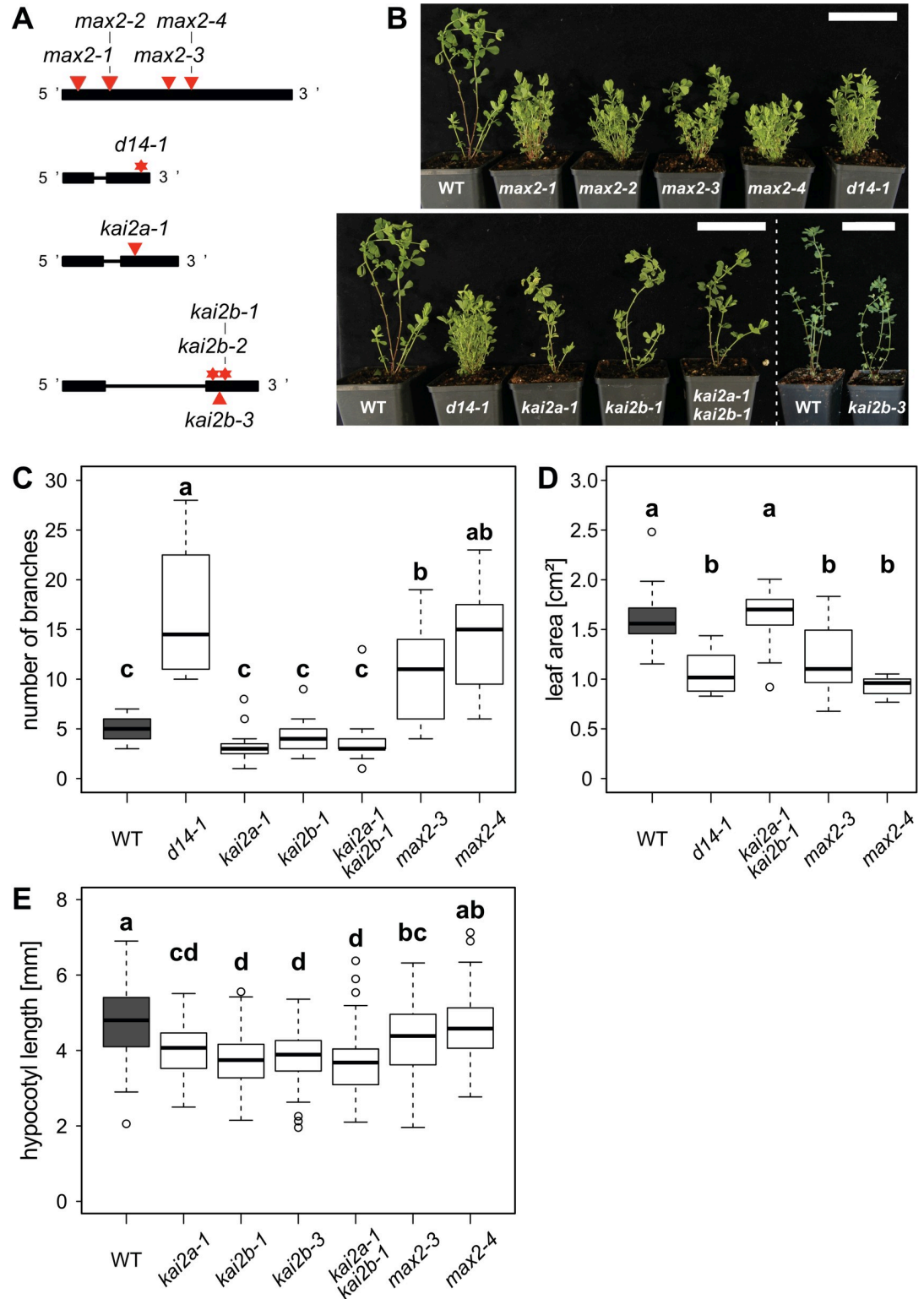


Fig 6. Role of D14, KAI2a, KAI2b and MAX2 in shoot and hypocotyl development of *Lotus japonicus*. (A) Schematic representation of the *L. japonicus* D14, KAI2a, KAI2b and MAX2 genes. Black boxes and lines show exons and introns, respectively. LORE1 insertions are indicated by red triangles and EMS mutations by red stars. (B) Shoot phenotype of *L. japonicus* wild-type and karrikin and strigolactone perception mutants at 8 weeks post germination (wpg). Scale bars: 7 cm. (C) Number of branches and of *L. japonicus* wild-type, karrikin and strigolactone perception mutants at 7 wpg (n = 12–21). (D)

Leaf size of the indicated genotypes at 9 wpg (n = 12–15 plants with an average of 3 leaves). (E) Hypocotyl length of the indicated genotypes of *L. japonicus* under short day conditions (8h light/16h dark) at 1 wpg (n = 79–97). (C–E) Letters indicate different statistical groups (ANOVA, post-hoc Tukey test).

<https://doi.org/10.1371/journal.pgen.1009249.g006>

perception for suppression of hypocotyl elongation under white light is not conserved in *L. japonicus* and/or that KL may not be produced under these growth conditions.

To examine whether *L. japonicus* hypocotyls are responsive to karrikin treatment, we measured the dose-response of hypocotyl growth in wild-type to KAR₁, KAR₂ and also to *rac*-GR24. Hypocotyl elongation of wild type plants was progressively inhibited with increasing concentrations of all three compounds (S10A Fig). However, it was not suppressed by KAR₁ or KAR₂ treatment in the *kai2a-1 kai2b-1* double mutant and the *max2-4* mutant (S10B and S10C Fig). This demonstrates that similar to Arabidopsis, the hypocotyl response to karrikin of *L. japonicus* depends on the KAI2-MAX2 receptor complex. We also examined the KAR₁ response of *kai2a* and *kai2b* single mutant hypocotyls and found that *kai2a-1* did not significantly respond to KAR₁ and KAR₂, while the two allelic *kai2b* mutants showed reduced hypocotyl growth in response to both karrikins (S10B Fig). The transcript accumulation pattern of *DLK2* (*Lj2g3v0765370*)—a classical karrikin marker gene in Arabidopsis [4,45]—was consistent with this observation and *DLK2* was induced in hypocotyls by KAR₁ and KAR₂ in a *LjKAI2a*-dependent but *LjKAI2b*-independent manner (S10D Fig). *rac*-GR24 treatment induced an increase of *DLK2* transcripts in a *LjKAI2b*-independent, partially *LjKAI2a*-dependent, and fully *MAX2*-dependent manner, suggesting that this induction is mediated via *LjKAI2a* (GR24^{ent-5DS}) and *LjD14* (GR24^{5DS}), similar to Arabidopsis [45] (S10C Fig). In summary, *LjKAI2a* appears to be necessary and sufficient to perceive karrikins and GR24^{ent-5DS} in the *L. japonicus* hypocotyl, possibly because expression of *LjKAI2b* in hypocotyls is too low under short day conditions (S2B Fig).

***L. japonicus* root system architecture is modulated by KAR₁ but not by KAR₂ treatment**

rac-GR24 treatment can trigger root system architecture changes in Arabidopsis and *Medicago truncatula* [57–59], and it has recently become clear for Arabidopsis that lateral and adventitious root formation is co-regulated by karrikin and strigolactone signaling [15,25]. We examined, whether *L. japonicus* root systems respond to *rac*-GR24, KAR₁ and KAR₂ (Fig 7A). Surprisingly, in contrast to Arabidopsis and *M. truncatula*, *L. japonicus* root systems responded neither to *rac*-GR24 nor to KAR₂. Only KAR₁ treatment led to a dose-dependent decrease in primary root length and an increase of post-embryonic root (PER) number, and thus to a higher PER density (Fig 7A, S12A Fig). PERs include lateral and adventitious roots that can be difficult to distinguish in *L. japonicus* seedlings grown on Petri dishes. The instability of *rac*-GR24 over time in the medium could potentially prevent a developmental response of the root to this compound in our experiments [60]. However, refreshing the medium with new *rac*-GR24 or karrikins at 5 days post-germination, did not alter the outcome (Fig 7B). Consistently, we observed *DLK2* induction in roots after KAR₁ but not after KAR₂ treatment (Fig 7C).

Together with the hypocotyl responses to KAR₁, KAR₂ and *rac*-GR24 this indicates organ-specific sensitivity or responsiveness to these three compounds in *L. japonicus* with a more stringent uptake, perception and/or response system in the root.

Surprisingly, we found that the roots responded to *rac*-GR24 treatment with increased *DLK2* transcript accumulation (Fig 7D) although no change in root architecture was observed in response to this treatment (Fig 7A). This suggests that different ligands may be transported

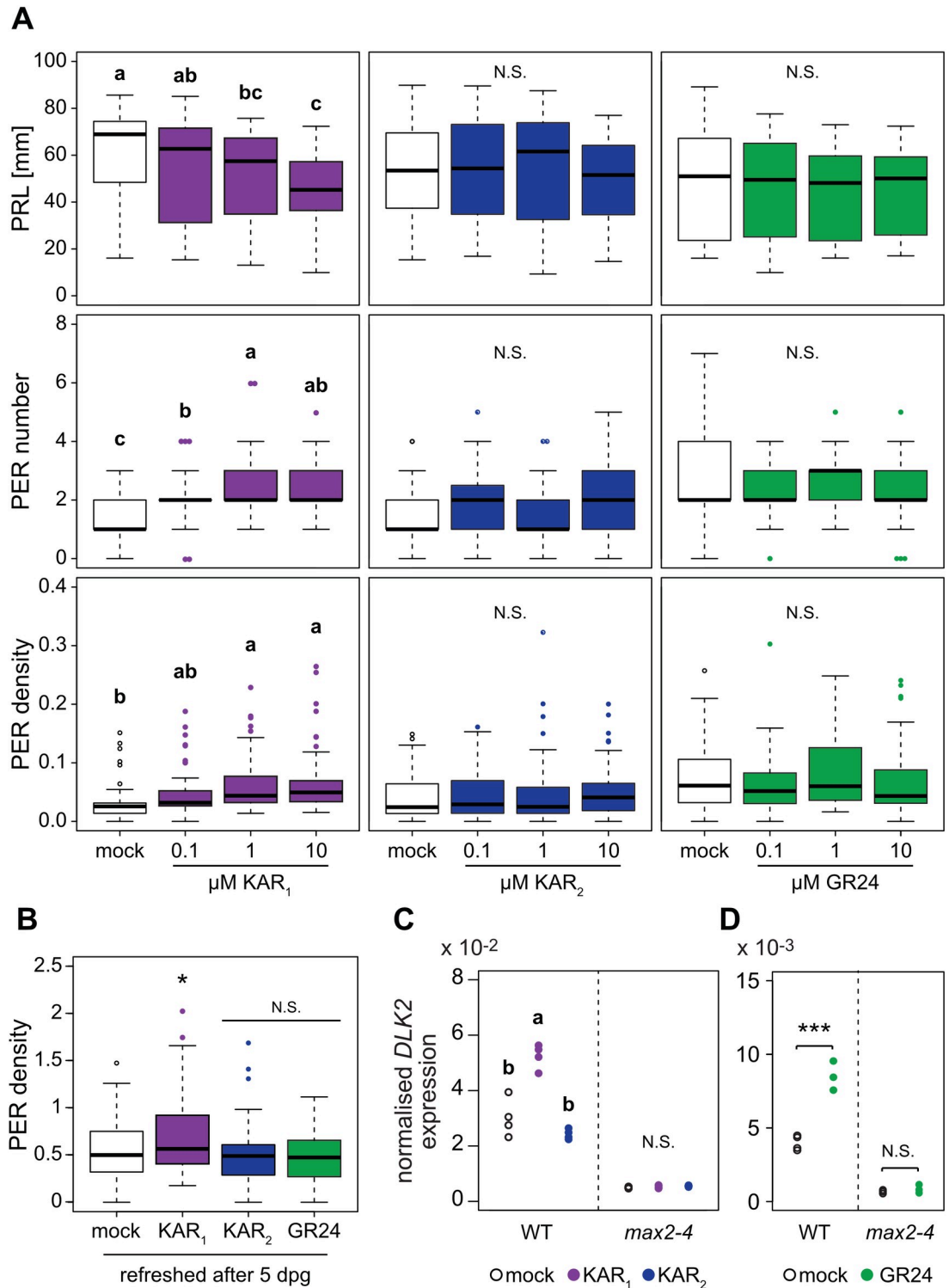


Fig 7. *Lotus japonicus* root system architecture is affected specifically by treatment with KAR₁ but not KAR₂. (A) Primary root length (PRL), post-embryonic root (PER) number and PER density of wild-type plants 2 wpg after treatment with solvent (M) or three different concentrations of KAR₁, KAR₂ or *rac*-GR24 (GR24) (n = 32–57). (B) PER density of wild-type plants at 2 wpg and treated with solvent (Mock) 1 μM KAR₁, 1 μM KAR₂, or 1 μM *rac*-GR24 (n = 43–51). Plants were transferred onto fresh hormone-containing medium after 5 days. (C-D) RT-qPCR-based expression of *DLK2* normalized to *Ubiquitin* expression in roots at 2 wpg after 2 hours treatment with solvent (Mock), (C) 1 μM KAR₁ and 1 μM KAR₂, (D) 1 μM *rac*-GR24 (n = 4) (A and C) Letters indicate different statistical groups (ANOVA, post-hoc Tukey test). (B) Asterisks indicate significant differences

(ANOVA, Dunnett test, N.S.>0.05, * \leq 0.05). (D) Asterisk indicate significant differences versus mock treatment (Welch t-test, * \leq 0.05, ** \leq 0.01, *** \leq 0.001).

<https://doi.org/10.1371/journal.pgen.1009249.g007>

to different tissues or may have a divergent impact on receptor conformation, thereby mediating different downstream responses. To confirm the contrasting responses of *L. japonicus* root systems to KAR₁ and *rac*-GR24, and to test whether they result from divergent molecular outputs, we examined transcriptional changes after one, two and six hours treatment of *L. japonicus* wild-type roots with KAR₁ and *rac*-GR24 using microarrays. Statistical analysis revealed a total number of 629 differentially expressed (DE) genes for KAR₁-treated and 232 genes for *rac*-GR24-treated roots (S2 Table). In agreement with previous reports from Arabidopsis and tomato [44,61,62] the magnitude of differential expression was low. Most of the DE genes upon KAR₁ and *rac*-GR24 treatment responded solely after 2h (S11 Fig). Interestingly, only a minority of 48 genes responded in the same direction in response to both KAR₁ and *rac*-GR24, while the majority of genes responded specifically to KAR₁ (580 DEGs) or *rac*-GR24 (169 DEGs). If *rac*-GR24 were to simply mimic the effect of KAR (GR24^{ent-5DS}) and SL (GR24^{5DS}) on roots, one would have expected a large overlap with KAR₁ responses, and in addition a number of non-overlapping DEGs, regulated through D14. In summary, the microarray experiment confirmed largely non-overlapping responses of *L. japonicus* root response to KAR₁ and *rac*-GR24.

Both *LjKAI2a* and *LjKAI2b* mediate root architecture-responses to KAR₁ but only *LjKAI2a* mediates *DLK2* expression in response to GR24^{ent-5DS}

To inspect which α/β -hydrolase receptor mediates the changes in *L. japonicus* root system architecture in response to KAR₁ treatment, we examined PER density in the karrikin receptor mutants. For the non-treated roots, PER density was significantly higher than wild type only for *kai2b-1* (Fig 8A), possibly caused by the reduced primary root length of this line (S13 Fig). The *Ljkai2a-1 kai2b-1* double mutant and the *max2-4* mutant did not respond to KAR₁ treatment with changes in root system architecture (Fig 8A, S12B–S12D Fig). With 1 μ M KAR₁, we obtained contradictory results for the single *kai2a* and *kai2b* mutants in independent experiments (S12B and S12D Fig). However, *kai2a* and *kai2b* single mutants but not the *kai2a kai2b* double mutant responded to a slightly higher concentration of 3 μ M KAR₁ (Fig 8A), indicating that *LjKAI2a* and *LjKAI2b* redundantly perceive KAR₁ (or a metabolite thereof) in *L. japonicus* roots. This pattern was mirrored by *DLK2* expression in roots: both *kai2a* and *kai2b* single mutants responded to KAR₁ with increased *DLK2* expression, while the *kai2a-1 kai2b-1* double mutant and the *max2-4* mutant did not respond (Fig 8B). Since *LjKAI2b* did not respond to GR24^{ent-5DS} *in vitro* as well as in the heterologous Arabidopsis background (Figs 4B and 5, S6 Fig), we examined its ability to mediate *DLK2* induction by GR24^{ent-5DS} in *L. japonicus* roots. Wild-type and *kai2b* mutant roots responded to GR24^{ent-5DS} with increased *DLK2* expression, but this was not the case for *kai2a* roots confirming that *LjKAI2b* cannot bind and mediate responses to GR24^{ent-5DS} (Fig 8C). In summary, *LjKAI2a* and *LjKAI2b* act redundantly in roots in mediating responses to KAR₁ but only *LjKAI2a* can perceive GR24^{ent-5DS}.

Discussion

Gene duplication followed by sub- or neofunctionalization is an important driver in the evolution of complex signaling networks and signaling specificities during the adaptation to new or diverse environments. In legumes, the karrikin receptor gene *KAI2* multiplied possibly during the whole genome duplication that occurred in the Papilionoidae before the diversification of

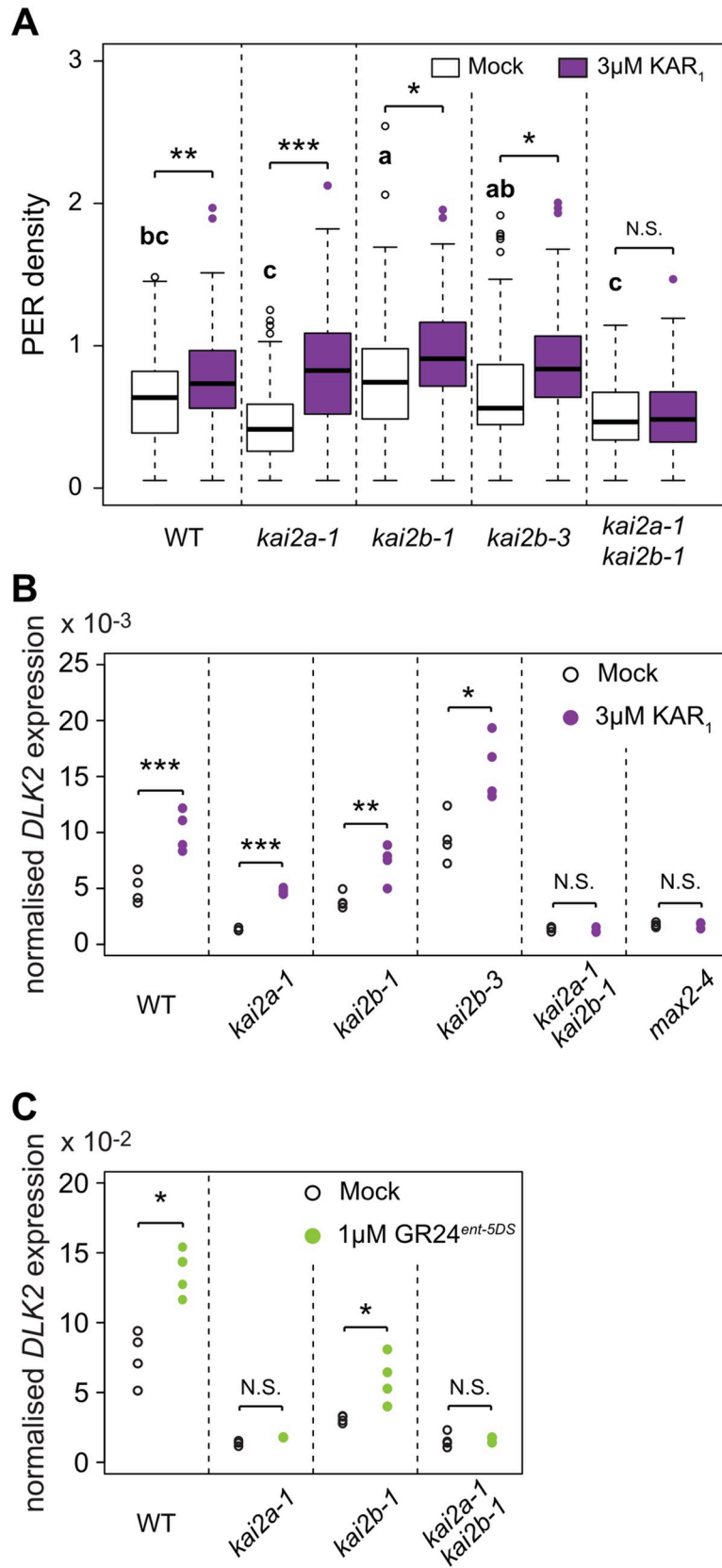


Fig 8. *LjKAI2a* and *LjKAI2b* operate redundantly in the response of roots to KAR₁ (A) Post-embryonic-root (PER) density of *L. japonicus* plants, 2 wpg after treatment with solvent (M) or 3 μ M KAR₁ (n = 34–72). Letters indicate different statistical groups only for non-treated mutant roots (ANOVA, post-hoc Tukey test). (B–C) RT-qPCR-based expression of *DLK2* in roots of *L. japonicus* plants at 2 wpg after 2 hours treatment with solvent (Mock) or (B) 3 μ M KAR₁ or (C) 1 μ M GR24^{ent-5DS}. Expression values were normalized to those of the housekeeping gene *Ubiquitin* (n = 3–4). (A–C) Asterisks indicate significant differences versus mock treatment (Welch t.test, * \leq 0.05, ** \leq 0.01, *** \leq 0.001).

<https://doi.org/10.1371/journal.pgen.1009249.g008>

legumes 59 million years ago [63]. While the Mimosoids, Genistoids and Millettoids, contain three different KAI2 versions, the Hologalegina clade appears to have lost one of them, retaining the more closely related *KAI2a* and *KAI2b* versions. Here, we provide evidence that *L. japonicus* *KAI2a* and *KAI2b* diversified in their ligand-binding specificity as well as their requirement in hypocotyl vs. root system responses to ligands (Fig 9).

LjKAI2a and *LjKAI2b* differ in their quantitative sensitivity to KAR₁ and KAR₂, which vary only by the presence of one methyl group in KAR₁ (Fig 3B). An increased hydrophobicity of the *LjKAI2b* binding pocket as compared to *LjKAI2a* may mediate the preference towards the more hydrophobic KAR₁, similar to the fire-following plant *Brassica tournefortii* [40]. The difference in ligand preference of *LjKAI2a* vs. *LjKAI2b* is more dramatic for GR24^{ent-5DS}, an enantiomer of the synthetic strigolactone analogue *rac*-GR24, which acts through Arabidopsis KAI2 when applied to plants, promotes interaction of KAI2 with SMAX1 in yeast and binds to *AtKAI2* *in vitro* [8,15,34,45,46]. We show that *LjKAI2a* mediates strong hypocotyl growth responses to GR24^{ent-5DS} in Arabidopsis as well as transcriptional activation of *DLK2* in *Lotus japonicus* roots. *LjKAI2b* is incapable of triggering these responses to the compound, while being able to induce the same responses upon KAR₁ treatment. The dramatic difference in the ability of *LjKAI2a* and *LjKAI2b* to bind GR24^{ent-5DS} is confirmed *in vitro* by DSF and intrinsic tryptophan fluorescence assays. Together, these results demonstrate that the individual α/β -fold hydrolase receptor is sufficient to explain ligand sensitivity *in planta*.

Identifying the determinants of ligand-binding specificity of D14 and different KAI2 and KAI2-like proteins is an area of active research. Binding specificity of D14 and KAI2 to SLs and KARs respectively has been associated with the geometry and size of the binding pocket [6,64]. Changes in amino acid residues located in the pocket of divergent KAI2 versions in parasitic weeds have enabled alterations in pocket architecture and evolution of a chimeric receptor that perceives strigolactones like D14 but mediates germination like KAI2 [38,39]. The rigidity of lid helices forming the tunnel of the binding pocket have been proposed to determine specificity of KAI2-like proteins for strigolactone-like molecules vs. KAR₁ in *Physcomitrella patens* [37].

We identified three amino acids at the ligand-binding pocket that differ between *LjKAI2a* and *LjKAI2b*. Two of these are conserved across the legume KAI2a and KAI2b clades, namely L160 and S190 in KAI2a and M161 and L191 in KAI2b. This pattern of conservation suggests functional relevance in maintaining flexibility for different KAI2 ligands in legumes. Indeed, exchanging these two amino acids slightly changes the thermal instability of the two KAI2 versions in the DSF assay. Neither of the two amino acid changes is predicted to substantially impact the pocket volume or geometry but the amino acids of *LjKAI2b* are more hydrophobic, which may explain the preference for the more hydrophobic KAR₁ over KAR₂. A similar phenomenon was observed in *Brassica tournefortii*, a fire-following weed that has two functional KAI2 genes [40]. Similar to the situation in *L. japonicus*, *BtKAI2b* mediated a greater sensitivity to KAR₁ over KAR₂ in the Arabidopsis background, while it was the reverse for *BtKAI2a*. This was explained by one amino acid polymorphism in the binding pocket towards a more hydrophobic amino acid (V98L) in *BtKAI2b*. Notably, this residue (V98L) is in a very different

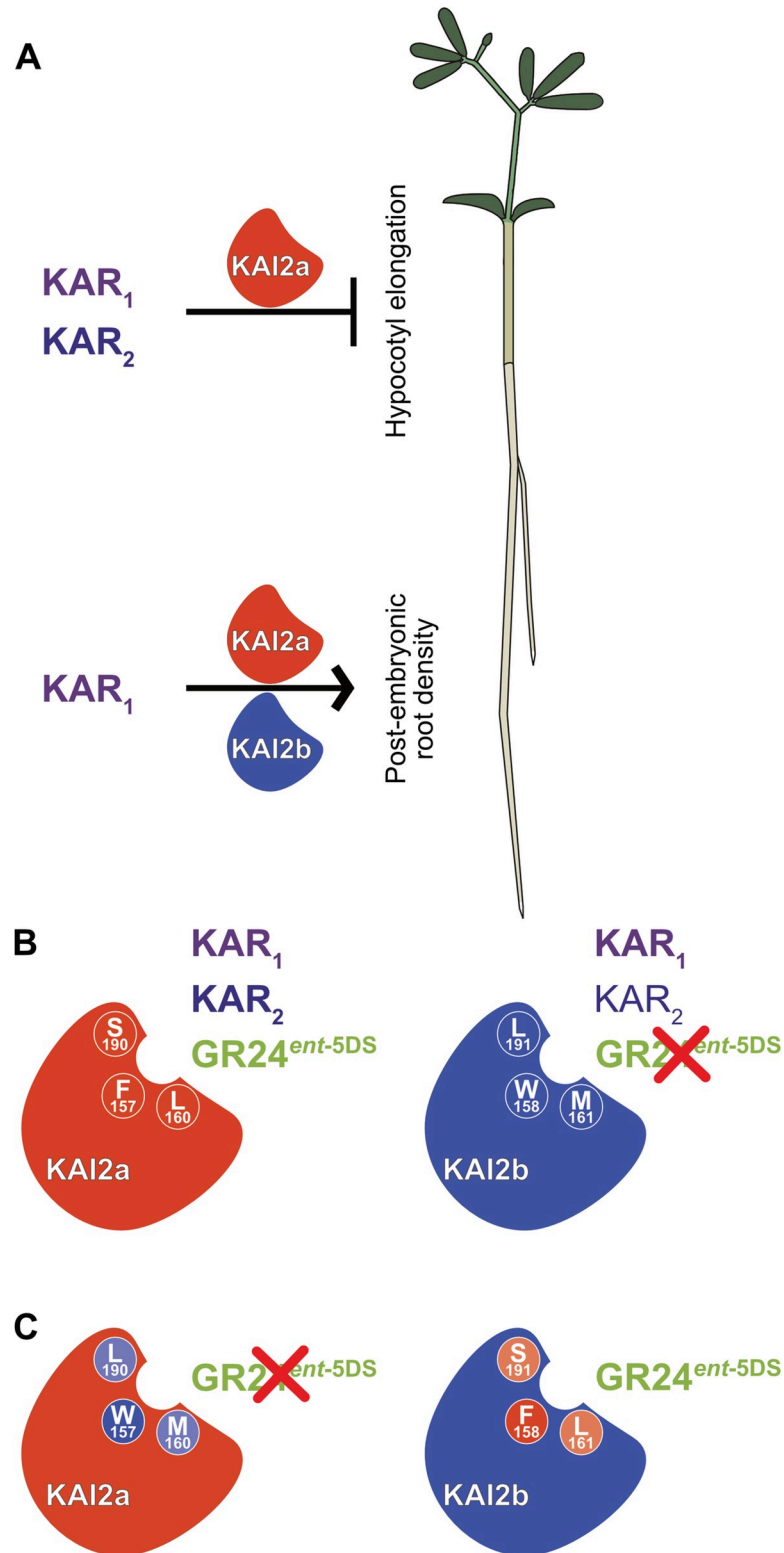


Fig 9. *L. japonicus* KAI2a and KAI2b display organ-specific redundancy and differ in their ligand-binding specificity. (A) *Lj*KAI2a is required to mediate inhibition of hypocotyl growth in response to KAR₁ and KAR₂. In roots *Lj*KAI2a and *Lj*KAI2b redundantly promote postembryonic root density, but only in response to KAR₁ treatment. (B) In the Arabidopsis *kai2-2* background *Lj*KAI2a mediates hypocotyl growth inhibition in response to KAR₁, KAR₂ and GR24^{ent-5DS}. In the same background, *Lj*KAI2b mediates a stronger response to KAR₁ than to KAR₂.

and no response to GR24^{ent-5DS} (indicated by a red cross). Three divergent amino acids at the binding pocket are indicated in white. (C) Swapping the three divergent amino acids in the binding pocket reconstitutes GR24^{ent-5DS} activity through *LjKAI2b* and abolishes GR24^{ent-5DS} activity through *LjKAI2a*. Among the three amino acids F157/W158 are decisive for GR24^{ent-5DS} binding (strong colors), while L160/M161 and S190/L191 play a weaker role (pale colors). Amino acids from *LjKAI2a* have a red/pale red and amino acids from *LjKAI2b* a violet/pale background.

<https://doi.org/10.1371/journal.pgen.1009249.g009>

position than the polymorphic residues in *L. japonicus* KAI2a/KAI2b, suggesting that the receptors are highly plastic and that similar binding-specificities for a given ligand may be achieved by changing hydrophobicity in different positions of the pocket.

Exchanging L160/M161 and S190/L191 between *L. japonicus* KAI2a and KAI2b was sufficient to change their sensitivity to GR24^{ent-5DS} in the DSF *in vitro* assay. However, the developmental response of Arabidopsis hypocotyls was hardly changed, possibly because *in vivo*, suboptimal ligand binding to the receptor can be stabilized by interacting proteins. A third amino acid difference (F157/W158) between the two KAI2 proteins occurs in *L. japonicus*. This residue critically determines sensitivity to GR24^{ent-5DS} *in vitro* as well as in Arabidopsis likely because the bulky tryptophan may sterically hinder GR24^{ent-5DS} binding, while still allowing binding of the smaller karrikins. In fact, swapping F157 with W158 alone was sufficient to swap the ability to respond to GR24^{ent-5DS} in DSF as well as intrinsic fluorescence assays.

B. tournefortii is a fire-following plant, the seeds of which respond to karrikins with dormancy breaking and germination [40]. Therefore, it makes adaptive sense for *B. tournefortii* to maintain two copies of KAI2, one of which is specialized for KAR₁, the most abundant KAR in smoke, and the other of which may be specialized for the endogenously produced ligand. For *L. japonicus*, which is not a fire-follower, KAR₁, KAR₂ and GR24^{ent-5DS} are likely not natural KAI2 ligands. Nevertheless, the maintenance of two KAI2 genes in the Hologalegina legumes, each with amino acid polymorphisms conferring differences in binding preferences to artificial ligands, requires an adaptive basis. One possibility is that *L. japonicus* KAI2a and KAI2b have specialized to bind different ligands *in planta*, indicative of legumes producing at least two different versions of the as-yet-unknown KAI2 ligand. The distinct expression patterns and developmental roles of *LjKAI2a* and *LjKAI2b* might also be consistent with a tissue-specific diversity of ligands, or even an endogenous ligand versus an exogenous ligand derived from the rhizosphere. From our assays with artificial ligands we extrapolate that *LjKAI2b* has a higher ligand selectivity than *LjKAI2a*. The additional amino acid change that occurred in *L. japonicus* but not in the other examined legumes may indicate that the KL bouquet of *L. japonicus* has further diversified. Alternatively, the F to W substitution in *LjKAI2b* may confer resistance to (a) toxic allelochemical(s) that may be released into the rhizosphere by competing plants or microorganisms. This speculative hypothesis is consistent with the role of *LjKAI2b* in roots (but not in hypocotyls) and with the observation that the F157W exchange occurred in several unrelated species independently that may all encounter compounds capable of blocking KAI2a in their natural habitat. It will be exciting to investigate the biological significance of this receptor sub-functionalization and the putative diversity of their ligands, once the molecule class of KL and its variants have been identified.

In addition to ligand-binding specificity at the level of the receptor, we identified a surprising organ-specific responsiveness to synthetic KAI2 ligands in *L. japonicus*. While hypocotyl growth is inhibited in response to KAR₁, KAR₂ and *rac*-GR24, root systems only respond to KAR₁ with architectural changes (Fig 9A). To our knowledge such an organ-specific discrimination of different but very similar KAR molecules has not previously so clearly been observed. However, a similar scenario could be at play in rice, in which transcriptome analysis of KAR₂-treated rice roots identified no differentially expressed gene [16], whereas rice mesocotyls

respond with growth inhibition to the same treatment [7,16]. Although KAI2 can be shown to bind KAR₁ *in vitro* by isothermal titration calorimetry or fluorescent microdialysis [5,6,65], there is evidence suggesting that KARs are not directly bound by KAI2 *in vivo*, but may be metabolized first to yield the correct KAI2-ligand, which may bind with higher affinity [34,46]. It is possible that substrate specificities differ among enzymes involved in KAR metabolism in hypocotyls vs. roots. This would imply that the single methyl group, which distinguishes KAR₁ from KAR₂, is sufficient to impact specialized metabolism of karrikins. Alternatively, the transport of KAR₂ or the KAR₂-derived metabolic product could be limited in the root system, or KAR₂-derivatives may be rapidly catabolised in roots, thus limiting their effect. While KAR₂ fails to induce increased PER density as well as *DLK2* expression in *L. japonicus* roots, GR24^{ent-5DS} triggers *DLK2* transcript accumulation albeit being unable to increase PER density. *DLK2* induction by GR24^{ent-5DS} requires KAI2a, thus involvement of D14 can be excluded. Furthermore, *LjKAI2a* and *LjKAI2b* act redundantly in mediating KAR₁-induced root system changes, excluding the possibility that they are regulated exclusively by *LjKAI2b*, which cannot bind GR24^{ent-5DS}. It is tempting to speculate that conformational changes of KAI2 proteins may differ depending on the ligand and that the extent of the change may influence the interaction strength with the karrikin signaling repressor SMAX1, MAX2 and/or additional proteins [8,66]. Perhaps *DLK2* expression is more sensitive to quantitative SMAX1 removal than genes required to be induced for root system changes, such as the ethylene biosynthesis gene *ACS7* [66]. Alternatively, SMAX1 proteins inhibiting *DLK2* expression are more accessible to the receptor complex, thereby allowing interaction even when the receptor binds a suboptimal ligand, as compared to SMAX1 individuals suppressing transcriptional activity of genes involved in root system changes; or GR24^{ent-5DS} is only taken up into a subset of cells, in which SMAX1 removal does not mediate root system changes.

We observed that KAR₁ treatment triggers increased PER density in *L. japonicus*. This is somewhat contradictory to *kai2* and *max2* mutants in *Arabidopsis*, which display an increased lateral root density [15]. The discrepancy may result from different physiological optima between the two species or from nutrient conditions in the two experimental systems. We observed the KAR₁ response of *L. japonicus* root systems in half-Hoagland solution with low phosphate levels (2.5 μM PO₄³⁻) and without sucrose, whereas the root assay in *Arabidopsis* was conducted in ATS medium (*Arabidopsis thaliana* salts) with 1% sucrose [15]. Phosphate and sucrose levels have previously been described to influence the effect of strigolactone and *rac*-GR24 on *Arabidopsis* root architecture [57,67,68].

In *Arabidopsis* and rice, KAI2/D14L is required to inhibit hypocotyl and mesocotyl elongation, respectively [3,4,16]. Since these two species are evolutionarily distant from each other, but have both retained a function of KL signaling in inhibiting the growth of similar organs, it seemed likely that this function would be conserved among a large number of plant species. Surprisingly, in *L. japonicus*, we observed no elongated hypocotyl phenotype for the *kai2a-1 kai2b-1* double and two allelic *max2* mutants (Fig 5). However, we could trigger a reduction of hypocotyl elongation by treatment with KAR₁, KAR₂ and *rac*-GR24 in the wild type and in a *LjKAI2a* and *LjMAX2*-dependent manner. Perhaps the endogenous KL levels in *L. japonicus* hypocotyls are insufficient to cause inhibition of hypocotyl elongation, at least under our growth conditions. Somewhat contradictory to the hypocotyl responsiveness to KAR₁, KAR₂ and *rac*-GR24 of wild type and *kai2b* mutants, untreated hypocotyls of both *L. japonicus kai2* mutants as well as *max2* mutants were slightly shorter than those of wild-type plants. We currently do not know the reason for this. Perhaps it is caused by small and undetectable differences in germination between the genotypes. It is difficult to precisely record germination rates of *L. japonicus* because seeds hardly germinate when they are not scarified, while scarification can abolish detectable differences in germination speed between mutants.

In summary, we have demonstrated sub-functionalization of two KAI2 copies in *L. japonicus* with regard to their ligand-binding specificity and organ-specific relevance. Furthermore, we find organ-specific responsiveness of *L. japonicus* to two artificial KAI2 ligands. A phenylalanine to tryptophan transition independently occurred in the KAI2-binding pocket in several angiosperms, while a leucine-to-methionine and a serine-to-leucine exchange are conserved in KAI2a and KAI2b across legumes. This conservation and independent multiple occurrence of specific amino acid polymorphisms suggests that they bear functional relevance for discriminating diverse KAI2 ligands. Our findings open novel research avenues towards understanding the diversity in KL ligand-receptor relationships and in developmental responses to, as yet, unknown natural as well as synthetic butenolides that influence diverse aspects of plant development.

Materials and methods

Plant material and seed germination

The *A. thaliana kai2-2* (Ler background) and *d14-1* (Col-0 background) mutants are from [4], the *d14-1 kai2-2* double mutant from [45], the *htl-2* mutant was provided by Min Ni [69] and the cross with K02821 is from [16]. Seeds were surface sterilized with 70% EtOH. For synchronizing the germination, seeds were placed on ½ MS 1% agar medium and maintained at 4°C in the dark for 72 hours.

The *L. japonicus* Gifu *max2-1*, *max2-2*, *max2-3*, *max2-4*, *kai2a-1* and *kai2b-3* mutations are caused by a LORE1 insertion. Segregating seed stocks for each insertion were obtained from the Lotus Base (<https://lotus.au.dk>, [70]) or Makoto Hayashi (NIAS, Tsukuba, Japan, [53] for *max2-2*). The *d14-1*, *kai2b-1* and *kai2b-2* mutants were obtained by TILLING [54] at RevGenUK (<https://www.jic.ac.uk/technologies/genomic-services/revgenuk-tilling-reverse-genetics/>). Homozygous mutants were identified by PCR using primers indicated in S3 Table. For germination, *L. japonicus* seeds were manually scarified with sand-paper and surface sterilized with 1% NaClO. Imbibed seeds were germinated on 1/2 Hoagland medium containing 2.5µM PO₄³⁻ and 0.4% Gelrite (www.duchefa-biochemie.com), at 24°C for 3 days in the dark, or on ½ MS 0.8% agar at 4°C for 3 days in dark (only for the experiment in Fig 6E).

Phylogenetic, synteny and protein sequence analysis

Lotus japonicus KAI2, D14 and MAX2 sequences were retrieved using tBLASTn with AtKAI2, AtD14 and AtMAX2, against the NCBI database, the plantGDB database and the *L. japonicus* genome V2.5 (<http://www.kazusa.or.jp/lotus>). The presence of MAX2-like was identified by tBLASTn in an in-house genome generated by next generation sequencing using CLC Main Workbench [71]. Pea sequences were found by BLASTn on “pisum sativum v2” database with AtKAI2 as query (<https://www.coolseasonfoodlegume.org>). For Fig 1, the MUSCLE alignment of the protein sequences was used to generate Maximum-likelihood tree with 1000 bootstrap replicates in MEGAX [72]. For the synteny analysis of MAX2 and MAX2-like, flanking sequences were retrieved from the same in-house genome [71]. For S7 Fig, KAI2 sequences across the plant phylogeny were retrieved by BLAST-P search against the EnsemblPlants, NCBI and 1KP databases [51], in addition, KAI2 sequences of the parasitic plants *Striga hermonthica* and *Orobancha cumana* were retrieved from Conn et al. 2015 [38]. The MUSCLE alignment, generated in MEGAX [72], was used to produce a tree with 1000 bootstrap replicates with IQTREE [73].

Structural homology modelling of proteins

Proteins were modelled using SWISS-MODEL tool (<https://swissmodel.expasy.org>) with the *A. thaliana* KAI2 (4JYM) templates [5].

Visualization of protein localization in *Nicotiana benthamiana* leaves and Western Blot

D14, *KAI2a*, *KAI2b* and *MAX2* genes were amplified from *L. japonicus* genomic DNA by Phusion PCR using the primers shown in S3 Table and cloned in pENTR/D-TOPO (Invitrogen). They were then transferred by LR reaction (Invitrogen) into Gateway plasmids (described in [74,75]) 35S:TSaphire-GW-Nos (for *MAX2* fusions) or 35S: mOrange-GW-Nos (for *D14*, *KAI2a*, *KAI2b* fusions). *Nicotiana benthamiana* leaves were transiently transformed by infiltration with *Agrobacterium tumefaciens* strain AGL1 containing the plasmids encoding TSaphire-MAX2, mOrange-D14, mOrange-KAI2a and mOrange-KAI2b fusion proteins. Three days after transformation transformed *N. benthamiana* leaf disks were cut and observed with an SP5 Confocal microscope (www.leica-microsystems.com). Overlays were generated using Fiji (<http://fiji.sc/>).

For Western Blots proteins were extracted from 3 pooled leaf disks according to Singh et al 2014 [74]. SDS page and protein blotting was performed as described [74]. Membranes were probed using anti-GFPmono monoclonal IgG from mouse (Roche) and anti-dsRed from mouse (Clontech) at a dilution 1:5000 and the secondary anti-mouse HRP antibody from Goat (Biomol).

Bacterial protein expression and purification

Full-length *L. japonicus* coding sequences were cloned into pE-SUMO Amp using primers in S3 Table. Clones were sequence-verified and transformed into Rosetta DE3 pLysS cells (Novagen). Subsequent protein expression and purification were performed as described previously [34], with the following modifications: the lysis and column wash buffers contained 10 mM imidazole, and a cobalt-charged affinity resin was used (TALON, Takara Bio).

Differential scanning fluorimetry

DSF assays were performed as described previously [34]. Assays were performed in 384-well format on a Roche LightCycler 480 II with excitation 498 nm and emission 640 nm (SYPRO Tangerine dye peak excitation at 490 nm). Raw fluorescence values were transformed by calculating the first derivative of fluorescence over temperature. These data were then imported into GraphPad Prism 8.0 software for plotting. Data presented are the mean of three super-replicates from the same protein batch; each super-replicate comprised four technical replicates at each ligand concentration. Experiments were performed at least twice.

Intrinsic tryptophan fluorescence (ITF) assay

The ITF assay was performed in 384-well format on a BMG Labtech CLARIOstar multimode plate reader, using black FLUOtrac microplates (Greiner 781076). Reactions (20 μ L) were set up in quadruplicate and contained 10 μ M protein, 20 mM HEPES pH 7.5, 150 mM NaCl, 1.25% (v/v) glycerol, and 0–500 μ M ligand. Ligands were initially prepared in DMSO at 20x concentration, and therefore reactions also contained 5% (v/v) DMSO. Ligands were dissolved in buffer (20 mM HEPES pH 7.5, 150 mM NaCl, 1.25% (v/v) glycerol) at 2x concentration immediately before use, of which 10 μ L per well was dispensed with a multichannel pipette. An equivalent volume of 2x solution of protein in buffer was prepared and then dispensed onto the plate using an Eppendorf Multipipette with a 0.1 mL tip. The plate was mixed at 120 rpm for 2 min, centrifuged at 500x g for 2 min, and then incubated in the dark for 20 min at room temperature. Fluorescence measurements were taken first with fixed wavelength filters (excitation 295/10 nm; longpass dichroic 325 nm; emission 360/20 nm), followed by the linear

variable filter monochromator for emission wavelength scans (excitation 295/10 nm, emission 334–400 nm, step width 2 nm, emission bandwidth 8 nm). Measurements were performed at 25°C using 17 flashes per well for fixed filters or 20 flashes per well for wavelength scans. Gain and focus settings were set empirically for each experimental run. Data were blank-corrected by subtraction of fluorescence values from an identical set of wells containing ligand and buffer but no protein. Data analysis was performed in Graphpad Prism v8.4. Best fit curves were generated from untransformed fluorescence readings using nonlinear regression and the in-built “One site—Total” model, with least squares regression as a fitting method and an asymmetrical (profile-likelihood) 95% confidence interval. As saturation was not reached, only ambiguous values for K_d were returned. For emission wavelength scans, fluorescence values at each wavelength were normalised by expressing as a percentage of the corresponding value from samples lacking ligand.

Plasmid generation

Genes and promoter regions were amplified using Phusion PCR according to standard protocols and using primers indicated in [S3 Table](#). Plasmids were constructed by Golden Gate cloning [76] as indicated in [S4 Table](#).

Plant transformation

kai2-2 and *d14-1* mutants were transformed by floral dip in *Agrobacterium tumefaciens* AGL1 suspension. Transgenic seedlings were selected by mCherry fluorescence and resistance to 20 µg/mL hygromycin B in growth medium. Experiments were performed using T2 or T3 generations, with transformed plants validated by mCherry fluorescence.

Shoot branching assay

A. thaliana and *L. japonicus* were grown for 4 and 7 weeks, respectively in soil in the greenhouse at 16h/8h light/dark cycles. Branches with length >1cm were counted, and the height of each plant was measured.

Hypocotyl elongation assay

A. thaliana seedlings were grown for 5 days on half-strength Murashige and Skoog (MS) medium containing 1% agar (BD). *L. japonicus* seedlings were grown for 6 days on half-strength Hoagland medium containing 2.5µM PO_4^{3-} and 0.4% Gelrite (www.duchefa-biochemie.com), or on half-strength MS containing 0.8% agar (only for experiment in [Fig 6D](#)). Plants were grown in long day conditions in 16h/8h light/dark cycles for [Fig 2A](#) and in short-day conditions in 8h/16h light/dark cycles for all other hypocotyl assays. For KARRIKIN, *rac*-GR24, GR24^{5DS} and GR24^{ent-5DS} treatments the medium was supplied with KAR₁ (www.olchemim.cz), KAR₂ (www.olchemim.cz), *rac*-GR24 (www.chiralix.com) GR24^{5DS} and GR24^{ent-5DS} (www.strigolab.eu) or equal amounts of the corresponding solvent as a control. KARRIKINS were solubilized in 75% methanol and *rac*-GR24 and the GR24 stereoisomers in 100% acetone, at 10mM stock solution. After high-resolution scanning, the hypocotyl length was measured with Fiji (<http://fiji.sc/>).

Root system architecture assay

L. japonicus germinated seeds were transferred onto new plates containing KAR₁ (www.olchemim.cz), KAR₂ (www.olchemim.cz), *rac*-GR24 (www.chiralix.com) or the corresponding solvent. KARRIKINS were solubilized in 75% methanol and *rac*-GR24 in 100% acetone, at 10 mM

stock solution. Plates were partially covered with black paper to keep the roots in the dark, and placed at 24°C with 16-h-light/8-h-dark cycles for 2 weeks. After high-resolution scanning, post-embryonic root number was counted and primary root length measured with Fiji (<http://fiji.sc/>).

Treatment for analysis of transcript accumulation

Seedling roots were placed in 1/2 Hoagland solution with 2.5 μM PO_4^{3-} containing 1 or 3 μM Karrikin₁ (www.olchemim.cz for qPCR analysis, synthesized according to [77] for microarray analysis), Karrikin₂ (www.olchemim.cz), *rac*-GR24 (www.chiralix.com) or equal amounts of the corresponding solvents for the time indicated in Figure legends and the roots were covered with black paper to keep them in the dark.

Microarray analysis

Three biological replicates were performed for each treatment. Root tissues were harvested, rapidly blotted dry and shock frozen in liquid nitrogen. RNA was extracted using the Spectrum Plant Total RNA Kit (www.sigmaldrich.com). RNA was quantified and evaluated for purity using a Nanodrop Spectrophotometer ND-100 (NanoDrop Technologies, Willington, DE) and Bioanalyzer 2100 (Agilent, Santa Clara, CA). For each sample, 500 ng of total RNA was used for the expression analysis of each sample using the Affymetrix GeneChip Lotus1a520343 (Affymetrix, Santa Clara, CA). Probe labeling, chip hybridization and scanning were performed according to the manufacturer's instructions for IVT Express Labeling Kit (Affymetrix). The Microarray raw data was normalized with the Robust Multiarray Averaging method (RMA) [78] using the Bioconductor [79] package "Methods for Affymetrix Oligonucleotide Arrays" (affy version 1.48.0) [80]. Control and rhizobial probesets were removed before statistical analysis. Differential gene expression was analyzed with the Bioconductor package "Linear Models for Microarray Data" (LIMMA version 3.26.8) [81]. The package uses linear models for parameter estimation and an empirical Bayes method for differential gene expression assessment [82]. P-values were adjusted due to multiple comparisons with the Benjamini-Hochberg correction (implemented in the LIMMA package). Probesets were termed as significantly differentially expressed, if their adjusted p-value was smaller than or equal to 0.01 and the fold change for at least one contrast showed a difference of at least 50%. To identify the corresponding gene models, the probeset sequences were used in a BLAST search against *L. japonicus* version 2.5 CDS and version 3.0 cDNA sequences (<http://www.kazusa.or.jp/lotus/>). If, based on the bitscore, multiple identical hits were found, we took the top hit in version 2.5 CDS as gene corresponding to the probe. For version 3.0 cDNA search we used the best hit, that was not located on chromosome 0, if possible. For probesets known to target chloroplast genes (probeset ID starting with Lj_), we preferred the best hit located on the chloroplast chromosome, if possible. Probeset descriptions are based on the info file of the *L. japonicus* Microarray chip provided by the manufacturer (Affymetrix).

qPCR analysis

Tissue harvest, RNA extraction, cDNA synthesis and qPCR were performed as described previously [71]. qPCR reactions were run on an iCycler (Bio-Rad, www.bio-rad.com) or on QuantStudio5 (Applied Biosystems, www.thermofisher.com). Expression values were calculated according to the $\Delta\Delta\text{Ct}$ method [83]. Expression values were normalized to the expression level of the housekeeping gene *Ubiquitin*. For each condition three to four biological replicates were performed. Primers are indicated in S4 Table.

Statistics

Statistical analyses were performed using Rstudio (www.rstudio.com) after log transformation for qPCR analysis. F- and p-values for all figures are provided in [S5 Table](#). Raw data are shown in [S1 Data](#).

Supporting information

S1 Fig. MAX2-like underwent pseudogenization. (A) Schematic representation of the syntenic regions containing the *MAX2* and *MAX2-like* loci in *L. japonicus*. Coloured arrows and black lines show exons and introns respectively. (B) Protein alignment of *LjMAX2*, *LjMAX2*-like and an artificial *LjMAX2*-like with a deletion of the thymine at the position 453 in the coding sequence (*LjMAX2*-like $\Delta T453$). Position of the nucleotide deletion is indicated in the translated sequence by a red triangle. Amino-acid conservation between *MAX2* and *MAX2*-like is indicated by a dark background.

(TIFF)

S2 Fig. Organ-specific accumulation of *D14*, *KAI2a*, *KAI2b* and *MAX2* transcripts. (A-C) Transcript accumulation in wild-type of *D14*, *KAI2a*, *KAI2b* and *MAX2* normalized to expression of *Ubiquitin*, in (A) leaf, stem, flower and root of plants grown in pots, and in (B) hypocotyl and roots of 1 wpg plants grown on Petri dishes in 8h light /16h dark cycles, and in (C) roots of 2 wpg plants grown on Petri dishes in 16h light/8h dark cycles (n = 3).

(TIFF)

S3 Fig. Subcellular localisation of *LjD14*, *LjKAI2a*, *LjKAI2b* and *LjMAX2* in *Nicotiana benthamiana* leaves. (A) Subcellular localization of *LjD14*, *LjKAI2a*, *LjKAI2b* and *LjMAX2* in *N. benthamiana* leaf epidermal cells. *LjD14*, *LjKAI2a* and *LjKAI2b* are N-terminally fused with mOrange. *LjMAX2* is N-terminally fused with T-Sapphire. Scale bars: 25 μm . (B) Western blot of protein extracts from *N. benthamiana*, showing that the mOrange tag fused with *LjD14*, *LjKAI2a* and *LjKAI2b* was not cleaved at detectable amounts.

(TIFF)

S4 Fig. SDS-PAGE of purified SUMO fusion proteins and DSF assay with GR24^{5DS}. (A) 200 pmol (approx. 8 μg) of purified proteins were separated by 12% SDS-PAGE containing 2,2,2-trichloroethanol as a visualization agent. Below each lane is the calculated protein size in kilodaltons. S, protein size standards (Precision Plus Dual Color Standards, Bio-Rad #1610394) with corresponding sizes in kDa shown on the left. Optimal exposures of recombinant proteins and size standards were taken separately under UV transillumination and red epi-illumination, respectively. The two images were merged in post-processing, and the junction between them is indicated by a vertical line. (B) DSF curves of purified SUMO fusion proteins of wild-type *LjKAI2a* and *LjKAI2b*, and versions with swapped amino acids *LjKAI2a*^{W157,M160,L190}, *LjKAI2b*^{F158,L161,S191}, *LjKAI2a*^{W157}, *LjKAI2b*^{F158}, at the indicated concentrations of GR24^{5DS}. The first derivative of the change of fluorescence was plotted against the temperature. Each curve is the arithmetic mean of four technical replicates. Peaks indicate the protein melting temperature. There is no ligand-induced thermal destabilisation consistent with no protein-ligand interaction.

(TIFF)

S5 Fig. Amino acid differences between the legume KAI2a and KAI2b clades. Protein sequence alignment of KAI2a and KAI2b homologs from the legumes *Lotus japonicus*, *Pisum sativum*, *Medicago truncatula* and *Glycine max*, in comparison with Arabidopsis KAI2 and rice D14L. Residues conserved within the KAI2a and KAI2b clades but different between these

clades are coloured in green and blue. Residues of the catalytic triad are coloured in red. A non-conserved tryptophan in *LjKAI2b* located in the protein cavity is coloured in violet. Yellow triangles indicate amino acid residues located in the ligand-binding cavity of the proteins. Orange triangles indicate the three amino acids responsible for differences in GR24^{ent-5DS}-binding between *LjKAI2a* and *LjKAI2b*.

(TIFF)

S6 Fig. Intrinsic tryptophan fluorescence assay confirms inability of *LjKAI2b* to interact with GR24^{ent-5DS}. Intrinsic tryptophan fluorescence of wild-type *LjKAI2a* and *LjKAI2b*, and protein versions with swapped amino acids *LjKAI2a*^{M160,L190}, *LjKAI2b*^{L161,S191}, *LjKAI2a*^{M160,L190,W157}, *LjKAI2b*^{L161,S191,F158}, *LjKAI2a*^{W157}, *LjKAI2b*^{F158} measured with (A) fixed wavelength filters (excitation 295/10 nm; longpass dichroic 325 nm; emission 360/20 nm) and (B) with a linear variable filter monochromator for emission wavelength scans (excitation 295/10 nm, emission 334–400 nm, step width 2 nm, emission bandwidth 8 nm) at the indicated GR24^{ent-5DS} concentrations.

(TIFF)

S7 Fig. The F157 to W replacement occurred multiple times in angiosperm KAI2 proteins. Phylogenetic tree of KAI2 proteins rooted with *A. thaliana* DLK2. The KAI2a and KAI2b clades in legumes are highlighted by red and blue branches. Monophyletic groups corresponding to a same order or clade are highlighted by coloured rectangular boxes. Amino-acids at the positions corresponding to AtKAI2 157, 160 and 190 are indicated with single-letter code. A black background indicates the presence of the most common residues in KAI2 proteins: F157, L160 and A190. A blue background indicates residues M160 and L190, conserved in legume KAI2b. A red background indicates S190, conserved in legume KAI2a. A green background indicates a W at position 157. A brown background indicates a different residue.

(TIFF)

S8 Fig. Transcript accumulation in the *L. japonicus* KAR and SL receptor mutants. (A) qRT-PCR based transcript accumulation of *LjKAI2a* and *LjKAI2b*, in roots of wild type and *kai2a-1*, *kai2b-1*, *kai2b-3*, *kai2a-1 kai2b-1* and *max2-4* as well as *LjMAX2* and *LjD14* in *max2-4* and *d14-1*, respectively (n = 4). Expression values were normalized to those of the housekeeping gene *Ubiquitin*. (B) *LjKAI2b* transcript accumulation in wild-type, *kai2b-1* (stop codon) and *kai2b-3* (LORE1 insertion) mutants by semi-quantitative RT-PCR using primer pairs located 5' and 3' of the mutations, as well as flanking (ML) the mutations. Transcript accumulation of the housekeeping gene *Ubiquitin* is also shown.

(TIFF)

S9 Fig. Characterisation of the *kai2a-1* allele. (A) Schematic representation of mis-splicing caused by the LORE1 insertion in the *kai2a-1* mutant. (B) cDNA alignment showing the absence of nucleotides 369 to 383 in the *kai2a-1* transcript, causing a deletion of amino acids 124 to 128 (orange). (C) Protein model of *LjKAI2a* based on the AtKAI2-KAR₁ complex 4JYM [5] showing KAR₁ in green, residues of the catalytic triad in red and the amino acids missing in a hypothetical *LjKAI2a-1* protein in orange. (D) Hypocotyl elongation at 6 dpG in Arabidopsis *kai2-2* mutants transgenically complemented with genomic and the cDNA of wild-type *LjKAI2a* and *Ljkai2a-1* driven by the AtKAI2 promoter (n = 75–106). Plants were grown in 8h light/16h dark cycles. Letters indicate different statistical groups (ANOVA, post-hoc Tukey test).

(TIFF)

S10 Fig. *Lotus japonicus* hypocotyls respond to KAR₁ and KAR₂ in a *LjKAI2a*- and *LjMAX2*-dependent manner. (A) Hypocotyls and (B) hypocotyl length of *L. japonicus* wild-

type seedling at 1 wpg after treatment with solvent (M) or three different concentrations of KAR₁, KAR₂ or *rac*-GR24 (GR24) (n = 95–105). Letters indicate different statistical groups (ANOVA, post-hoc Tukey test). (C) Hypocotyl length of the indicated genotypes at 1 wpg after treatment with solvent (Mock), 1 μM KAR₁ or 1 μM KAR₂ (n = 73–107). (D) Hypocotyl length of wild-type and *max2-4* seedlings 1 wpg after treatment with solvent (Mock), 1 μM KAR₁, 1 μM KAR₂ (n = 66–96). (E) RT-qPCR-based expression of *DLK2* in hypocotyls at 1 wpg after 2 hours treatment with solvent (Mock), 1 μM KAR₁, 1 μM KAR₂, or 1 μM *rac*-GR24 (GR24) (n = 3). Expression values were normalized to those of the housekeeping gene *Ubiquitin*. (A–E) Seedlings were grown in 8h light/16h dark cycles. (C–E) Asterisks indicate significant differences of the compounds versus mock treatment (ANOVA, post-hoc Dunnett test, N.S.>0.05, *≤0.05, **≤0.01, ***≤0.001).

(TIFF)

S11 Fig. Small overlap between transcriptional responses of *Lotus japonicus* roots to KAR₁ and *rac*-GR24. Number of differentially expressed genes (DEGs, adjusted p-value < 0.01) as assessed by microarray analysis. Left panel: DEGs responding to 1 μM KAR₁ after 1h, 2h and 6h incubation. Middle panel: DE genes responding to 1 μM *rac*-GR24 1h, 2, 6h incubation. Right panel: comparison of DE genes responding to 2 h treatment with KAR₁ and *rac*-GR24.

(TIFF)

S12 Fig. KAR perception mutants are less responsive to KAR₁ treatment. (A) Image of *Lotus japonicus* seedling with indicated post-embryonic roots (PERs). (B–D) Post-embryonic-root (PER) density of *L. japonicus* plants, 2 wpg after treatment with solvent (Mock) or 1 μM KAR₁, of wild-type, (B) *kai2a-1*, *kai2b-1* and *kai2a-1 kai2b-1* (n = 32–50); (C) *max2-4* (n = 34–43); (D) *kai2a-1*, *kai2b-3* and *kai2a-1 kai2b-1* (n = 37–72). (B–D) Asterisks indicate significant differences versus mock treatment (Welch t.test, *≤0.05, **≤0.01, ***≤0.001).

(TIFF)

S13 Fig. KAR₁ response in roots requires *LjKAI2a* or *LjKAI2b* and *LjMAX2*. Primary-root length (PRL) and post-embryonic-root (PER) number of *L. japonicus* plants, 2 wpg after treatment with solvent (Mock) or 3 μM KAR₁ (n = 34–72) displayed in Fig 9A. Asterisks indicate significant differences versus mock treatment (Welch t.test, *≤0.05, **≤0.01, ***≤0.001).

(TIFF)

S1 Table. *L. japonicus* mutants used in this study and information on seed production.

(DOCX)

S2 Table. Microarray-based differentially expressed genes in *Lotus japonicus* wild-type roots after 1h, 2h and 6h of treatment with 1μM KAR₁ or 1μM *rac*-GR24.

(XLSX)

S3 Table. Primers.

(DOCX)

S4 Table. Plasmids.

(DOCX)

S5 Table. Results of ANOVA for multiple comparisons.

(DOCX)

S1 Data. Raw data for all quantitative assays shown in the manuscript (except microarray data).

(XLSX)

Acknowledgments

We thank Andreas Keymer and Priya Pimprikar for cDNAs from root, flower, leaf and stem; and Verena Klingl for excellent technical support. We thank Martin Parniske (LMU Munich, Germany) for providing microarray chips and for setting up the *L. japonicus* mutant collection at the Sainsbury laboratory Norwich, UK; to Jens Stougaard and all scientists at LotusBase for the LORE1 insertion lines (University of Aarhus, Denmark); and to David Nelson (University of California Riverside, USA) for fruitful discussion. We thank Min Ni (University of Minnesota, USA) for seeds of the *A. thaliana htl-2* mutant.

Author Contributions

Conceptualization: Samy Carbonnel, Salar Torabi, Mark T. Waters, Caroline Gutjahr.

Data curation: Samy Carbonnel, Salar Torabi, Maximilian Griesmann, Mark T. Waters.

Formal analysis: Samy Carbonnel, Salar Torabi, Maximilian Griesmann, Mark T. Waters, Caroline Gutjahr.

Funding acquisition: Mark T. Waters, Caroline Gutjahr.

Investigation: Samy Carbonnel, Salar Torabi, Elias Bleek, Yuhong Tang, Stefan Buchka, Veronica Basso, Mark T. Waters, Caroline Gutjahr.

Methodology: Samy Carbonnel.

Project administration: Caroline Gutjahr.

Resources: Mitsuru Shindo, François-Didier Boyer, Trevor L. Wang, Michael Udvardi.

Supervision: Caroline Gutjahr.

Visualization: Samy Carbonnel, Salar Torabi.

Writing – original draft: Samy Carbonnel, Caroline Gutjahr.

Writing – review & editing: Caroline Gutjahr.

References

1. Flematti GR, Ghisalberti EL, Dixon KW, Trengove RD. A compound from smoke that promotes seed germination. *Science*. 2004; 305(5686):977. <https://doi.org/10.1126/science.1099944> PMID: 15247439
2. Nelson DC, Riseborough JA, Flematti GR, Stevens J, Ghisalberti EL, Dixon KW, et al. Karrikins discovered in smoke trigger Arabidopsis seed germination by a mechanism requiring gibberellic acid synthesis and light. *Plant Physiol*. 2009; 149(2):863–73. <https://doi.org/10.1104/pp.108.131516> PMID: 19074625
3. Nelson DC, Scaffidi A, Dun EA, Waters MT, Flematti GR, Dixon KW, et al. F-box protein MAX2 has dual roles in karrikin and strigolactone signaling in *Arabidopsis thaliana*. *Proc Natl Acad Sci USA*. 2011; 108(21):8897–902. <https://doi.org/10.1073/pnas.1100987108> PMID: 21555559
4. Waters MT, Nelson DC, Scaffidi A, Flematti GR, Sun YK, Dixon KW, et al. Specialisation within the DWARF14 protein family confers distinct responses to karrikins and strigolactones in Arabidopsis. *Development*. 2012; 139(7):1285–95. <https://doi.org/10.1242/dev.074567> PMID: 22357928
5. Guo Y, Zheng Z, La Clair JJ, Chory J, Noel JP. Smoke-derived karrikin perception by the α/β -hydrolase KAI2 from Arabidopsis. *Proc Natl Acad Sci U S A*. 2013; 110(20):8284–9. <https://doi.org/10.1073/pnas.1306265110> PMID: 23613584
6. Kagiyama M, Hirano Y, Mori T, Kim SY, Kyojuka J, Seto Y, et al. Structures of D14 and D14L in the strigolactone and karrikin signaling pathways. *Genes Cells*. 2013; 18(2):147–60. Epub 2013/01/11. <https://doi.org/10.1111/gtc.12025> PMID: 23301669
7. Zheng J, Hong K, Zeng L, Wang L, Kang S, Qu M, et al. Karrikin signaling acts parallel to and additively with strigolactone signaling to regulate rice mesocotyl elongation in darkness. *Plant Cell*. 2020. Epub 2020/07/16. <https://doi.org/10.1105/tpc.20.00123> PMID: 32665307

8. Khosla A, Morffy N, Li Q, Faure L, Chang SH, Yao J, et al. Structure-function analysis of SMAX1 reveals domains that mediate its karrikin-induced proteolysis and interaction with the receptor KAI2. *Plant Cell*. 2020; 32(8):2639–59. Epub 2020/05/22. <https://doi.org/10.1105/tpc.19.00752> PMID: 32434855
9. Toh S, Holbrook-Smith D, Stokes ME, Tsuchiya Y, McCourt P. Detection of parasitic plant suicide germination compounds using a high-Throughput Arabidopsis HTL/KAI2 strigolactone perception system. *Chem & Biol*. 2014; 21(9):1253. <https://doi.org/10.1016/j.chembiol.2014.07.005> PMID: 25126711
10. Hrdlička J, Gucký T, Novák O, Kulkarni M, Gupta S, van Staden J, et al. Quantification of karrikins in smoke water using ultra-high performance liquid chromatography–tandem mass spectrometry. *Plant Methods*. 2019; 15(1):81. <https://doi.org/10.1186/s13007-019-0467-z> PMID: 31372177
11. Nelson DC, Flematti GR, Ghisalberti EL, Dixon KW, Smith SM. Regulation of seed germination and seedling growth by chemical signals from burning vegetation. *Annu Rev Plant Biol*. 2012; 63:107–30. Epub 2012/03/13. <https://doi.org/10.1146/annurev-arplant-042811-105545> PMID: 22404467
12. Conn CE, Nelson DC. Evidence that KARRIKIN-INSENSITIVE2 (KAI2) receptors may perceive an unknown signal that is not karrikin or strigolactone. *Front Plant Sci*. 2016; 6:1219. Epub 2016/01/19. <https://doi.org/10.3389/fpls.2015.01219> PMID: 26779242
13. Li W, Nguyen KH, Chu HD, Ha CV, Watanabe Y, Osakabe Y, et al. The karrikin receptor KAI2 promotes drought resistance in *Arabidopsis thaliana*. *PLoS Genet*. 2017; 13(11):e1007076. Epub 2017/11/14. <https://doi.org/10.1371/journal.pgen.1007076> PMID: 29131815
14. Swarbreck SM, Guerringue Y, Matthus E, Jamieson FJC, Davies JM. Impairment in karrikin but not strigolactone sensing enhances root skewing in *Arabidopsis thaliana*. *Plant J*. 2019;(98):607–21. Epub 2019/01/20. <https://doi.org/10.1111/tpj.14233> PMID: 30659713
15. Villacija Aguilar JA, Hamon-Josse M, Carbonnel S, kretschar A, Schmid C, Dawid C, et al. *SMAX1/SMXL2* regulate root and root hair development downstream of KAI2-mediated signaling in *Arabidopsis*. *PLoS Genet*. 2019; 15(8):1–27. <https://doi.org/10.1371/journal.pgen.1008327> PMID: 31465451
16. Gutjahr C, Gobbato E, Choi J, Riemann M, Johnston MG, Summers W, et al. Rice perception of symbiotic arbuscular mycorrhizal fungi requires the karrikin receptor complex. *Science*. 2015; 350(6267):1521–4. <https://doi.org/10.1126/science.aac9715> PMID: 26680197
17. Choi J, Lee T, Cho J, Servante EK, Pucker B, Summers W, et al. The negative regulator SMAX1 controls mycorrhizal symbiosis and strigolactone biosynthesis in rice. *Nat Commun*. 2020; 11(1):2114. Epub 2020/05/02. <https://doi.org/10.1038/s41467-020-16021-1> PMID: 32355217
18. Sun YK, Flematti GR, Smith SM, Waters MT. Reporter gene-facilitated detection of compounds in *Arabidopsis* leaf extracts that activate the karrikin signaling pathway. *Front Plant Sci*. 2016; 7:1799. Epub 2016/12/21. <https://doi.org/10.3389/fpls.2016.01799> PMID: 27994609
19. Cook CE, Whichard LP, Turner B, Wall ME, Egley GH. Germination of witchweed (*Striga lutea* Lour.): isolation and properties of a potent stimulant. *Science*. 1966; 154(3753):1189–90. <https://doi.org/10.1126/science.154.3753.1189> PMID: 17780042
20. Akiyama K, Matsuzaki K, Hayashi H. Plant sesquiterpenes induce hyphal branching in arbuscular mycorrhizal fungi. *Nature*. 2005; 435(7043):824–7. <https://doi.org/10.1038/nature03608> PMID: 15944706
21. Besserer A, Puech-Pages V, Kiefer P, Gomez-Roldan V, Jauneau A, Roy S, et al. Strigolactones stimulate arbuscular mycorrhizal fungi by activating mitochondria. *PLoS Biol*. 2006; 4(7):e226. Epub 2006/06/22. <https://doi.org/10.1371/journal.pbio.0040226> PMID: 16787107
22. Gomez-Roldan V, Fermas S, Brewer PB, Puech-Pages V, Dun EA, Pillot JP, et al. Strigolactone inhibition of shoot branching. *Nature*. 2008; 455(7210):189–94. <https://doi.org/10.1038/nature07271> PMID: 18690209
23. Umehara M, Hanada A, Yoshida S, Akiyama K, Arite T, Takeda-Kamiya N, et al. Inhibition of shoot branching by new terpenoid plant hormones. *Nature*. 2008; 455(7210):195–200. <https://doi.org/10.1038/nature07272> PMID: 18690207
24. Agusti J, Herold S, Schwarz M, Sanchez P, Ljung K, Dun EA, et al. Strigolactone signaling is required for auxin-dependent stimulation of secondary growth in plants. *Proc Natl Acad Sci U S A*. 2011; 108(50):20242–7. Epub 2011/11/30. <https://doi.org/10.1073/pnas.1111902108> PMID: 22123958
25. Swarbreck SM, Mohammad-Sidik A, Davies JM. Common components of the strigolactone and karrikin signaling pathways suppress root branching in *Arabidopsis thaliana*. *Plant Physiol*. 2020. Epub 2020/07/22. <https://doi.org/10.1104/pp.19.00687> PMID: 32690756
26. Hamiaux C, Drummond RS, Janssen BJ, Ledger SE, Cooney JM, Newcomb RD, et al. DAD2 is an alpha/beta hydrolase likely to be involved in the perception of the plant branching hormone, strigolactone. *Curr Biol*. 2012; 22(21):2032–6. Epub 2012/09/11. <https://doi.org/10.1016/j.cub.2012.08.007> PMID: 22959345

27. Waters MT, Scaffidi A, Flematti GR, Smith SM. Substrate-induced degradation of the alpha/beta-fold hydrolase KARRIKIN INSENSITIVE2 requires a functional catalytic triad but is independent of MAX2. *Mol Plant*. 2015; 8(5):814–7. <https://doi.org/10.1016/j.molp.2014.12.020> PMID: 25698586
28. Soundappan I, Bennett T, Morffy N, Liang Y, Stanga JP, Abbas A, et al. SMAX1-LIKE/D53 family members enable distinct MAX2-dependent responses to strigolactones and karrikins in *Arabidopsis*. *Plant Cell*. 2015; 27(11):3143–59. <https://doi.org/10.1105/tpc.15.00562> PMID: 26546447
29. Wang L, Wang B, Jiang L, Liu X, Li X, Lu Z, et al. Strigolactone signaling in *Arabidopsis* regulates shoot development by targeting D53-Like SMXL repressor proteins for ubiquitination and degradation. *Plant Cell*. 2015; 27(11):3128–42. <https://doi.org/10.1105/tpc.15.00605> PMID: 26546446
30. Zhou F, Lin Q, Zhu L, Ren Y, Zhou K, Shabek N, et al. D14-SCF(D3)-dependent degradation of D53 regulates strigolactone signaling. *Nature*. 2013; 504(7480):406–10. <https://doi.org/10.1038/nature12878> PMID: 24336215
31. Jiang L, Liu X, Xiong G, Liu H, Chen F, Wang L, et al. DWARF 53 acts as a repressor of strigolactone signaling in rice. *Nature*. 2013; 504(7480):401–5. <https://doi.org/10.1038/nature12870> PMID: 24336200
32. Bythell-Douglas R, Rothfels CJ, Stevenson DWD, Graham SW, Wong GK, Nelson DC, et al. Evolution of strigolactone receptors by gradual neo-functionalization of KAI2 paralogues. *BMC Biol*. 2017; 15(1):52. <https://doi.org/10.1186/s12915-017-0397-z> PMID: 28662667
33. Végh A, Incze N, Fábrián A, Huo H, Bradford KJ, Balázs E, et al. Comprehensive analysis of *DWARF14-LIKE2 (DLK2)* reveals its functional divergence from strigolactone-related paralogs. *Front Plant Sci*. 2017; 8(1641):1–14. <https://doi.org/10.3389/fpls.2017.01641> PMID: 28970845
34. Waters MT, Scaffidi A, Moulin SL, Sun YK, Flematti GR, Smith SM. A *Selaginella moellendorffii* ortholog of KARRIKIN INSENSITIVE2 functions in *Arabidopsis* development but cannot mediate responses to karrikins or strigolactones. *Plant Cell*. 2015; 27(7):1925–44. <https://doi.org/10.1105/tpc.15.00146> PMID: 26175507
35. Waters MT, Gutjahr C, Bennett T, Nelson DC. Strigolactone signaling and evolution. *Annu Rev Plant Biol*. 2017; 68:291–322. <https://doi.org/10.1146/annurev-arplant-042916-040925> PMID: 28125281
36. Lopez-Raez JA, Charnikhova T, Gomez-Roldan V, Matusova R, Kohlen W, De Vos R, et al. Tomato strigolactones are derived from carotenoids and their biosynthesis is promoted by phosphate starvation. *New Phytol*. 2008; 178(4):863–74. Epub 2008/03/19. <https://doi.org/10.1111/j.1469-8137.2008.02406.x> PMID: 18346111
37. Bürger M, Mashiguchi K, Lee HJ, Nakano M, Takemoto K, Seto Y, et al. Structural basis of karrikin and non-natural strigolactone perception in *Physcomitrella patens*. *Cell Rep*. 2019; 26(4):855–65. <https://doi.org/10.1016/j.celrep.2019.01.003> PMID: 30673608
38. Conn CE, Bythell-Douglas R, Neumann D, Yoshida S, Whittington B, Westwood JH, et al. Convergent evolution of strigolactone perception enabled host detection in parasitic plants. *Science*. 2015; 349(6247):540–3. <https://doi.org/10.1126/science.aab1140> PMID: 26228149
39. Toh S, Holbrook-Smith D, Stogios PJ, Onopriyenko O, Lumba S, Tsuchiya Y, et al. Structure-function analysis identifies highly sensitive strigolactone receptors in *Striga*. *Science*. 2015; 350(6257):203–7. Epub 2015/10/10. <https://doi.org/10.1126/science.aac9476> PMID: 26450211
40. Sun YK, Yao J, Scaffidi A, Melville KT, Davies SF, Bond CS, et al. Divergent receptor proteins confer responses to different karrikins in two ephemeral weeds. *Nat Commun*. 2020; 11(1):1264. Epub 2020/03/11. <https://doi.org/10.1038/s41467-020-14991-w> PMID: 32152287
41. Wojciechowski MF, Lavin M, Sanderson MJ. A phylogeny of legumes (Leguminosae) based on analysis of the plastid *matK* gene resolves many well-supported subclades within the family. *American J Bot*. 2004; 91(11):1846–62. <https://doi.org/10.3732/ajb.91.11.1846> PMID: 21652332
42. Shen H, Luong P, Huq E. The F-box protein MAX2 functions as a positive regulator of photomorphogenesis in *Arabidopsis*. *Plant Physiol*. 2007; 145(4):1471–83. <https://doi.org/10.1104/pp.107.107227> PMID: 17951458
43. Stirnberg P, Furner IJ, Ottoline Leyser HM. MAX2 participates in an SCF complex which acts locally at the node to suppress shoot branching. *Plant J*. 2007; 50(1):80–94. <https://doi.org/10.1111/j.1365-313X.2007.03032.x> PMID: 17346265
44. Nelson DC, Flematti GR, Riseborough JA, Ghisalberti EL, Dixon KW, Smith SM. Karrikins enhance light responses during germination and seedling development in *Arabidopsis thaliana*. *Proc Natl Acad Sci USA*. 2010; 107(15):7095–100. <https://doi.org/10.1073/pnas.0911635107> PMID: 20351290
45. Scaffidi A, Waters MT, Sun YK, Skelton BW, Dixon KW, Ghisalberti EL, et al. Strigolactone hormones and their stereoisomers signal through two related receptor proteins to induce different physiological responses in *Arabidopsis*. *Plant Physiol*. 2014; 165(3):1221–32. <https://doi.org/10.1104/pp.114.240036> PMID: 24808100

46. Wang L, Xu Q, Yu H, Ma H, Li X, Yang J, et al. Strigolactone and karrikin signaling pathways elicit ubiquitination and proteolysis of SMXL2 to regulate hypocotyl elongation in Arabidopsis. *Plant Cell*. 2020; 32(7):2251–70. Epub 2020/05/03. <https://doi.org/10.1105/tpc.20.00140> PMID: 32358074
47. Yao J, Mashiguchi K, Scaffidi A, Akatsu T, Melville KT, Morita R, et al. An allelic series at the *KARRIKIN INSENSITIVE 2* locus of *Arabidopsis thaliana* decouples ligand hydrolysis and receptor degradation from downstream signaling. *Plant J*. 2018; 96(1):75–89. Epub 2018/07/10. <https://doi.org/10.1111/tpj.14017> PMID: 29982999
48. Abe S, Sado A, Tanaka K, Kisugi T, Asami K, Ota S, et al. Carlactone is converted to carlactonoic acid by MAX1 in Arabidopsis and its methyl ester can directly interact with AtD14 in vitro. *Proc Natl Acad Sci U S A*. 2014; 111(50):18084–9. Epub 2014/11/27. <https://doi.org/10.1073/pnas.1410801111> PMID: 25425668
49. de Saint Germain A, Retailleau P, Norsikian S, Servajean V, Pelissier F, Steinmetz V, et al. Contalactone, a contaminant formed during chemical synthesis of the strigolactone reference GR24 is also a strigolactone mimic. *Phytochemistry*. 2019; 168:112112. Epub 2019/09/10. <https://doi.org/10.1016/j.phytochem.2019.112112> PMID: 31499274
50. Seto Y, Yasui R, Kameoka H, Tamiru M, Cao M, Terauchi R, et al. Strigolactone perception and deactivation by a hydrolase receptor DWARF14. *Nat Commun*. 2019; 10(1):191. Epub 2019/01/16. <https://doi.org/10.1038/s41467-018-08124-7> PMID: 30643123
51. Leebens-Mack JH, Barker MS, Carpenter EJ, Deyholos MK, Gitzendanner MA, Graham SW, et al. One thousand plant transcriptomes and the phylogenomics of green plants. *Nature*. 2019; 574(7780):679–85. <https://doi.org/10.1038/s41586-019-1693-2> PMID: 31645766
52. Malolepszy A, Mun T, Sandal N, Gupta V, Dubin M, Urbanski D, et al. The *LORE1* insertion mutant resource. *Plant J*. 2016; 88(2):306–17. <https://doi.org/10.1111/tpj.13243> PMID: 27322352
53. Fukai E, Soyano T, Umehara Y, Nakayama S, Hirakawa H, Tabata S, et al. Establishment of a *Lotus japonicus* gene tagging population using the exon-targeting endogenous retrotransposon *LORE1*. *Plant J*. 2012; 69(4):720–30. <https://doi.org/10.1111/j.1365-313X.2011.04826.x> PMID: 22014259
54. Perry JA, Wang TL, Welham TJ, Gardner S, Pike JM, Yoshida S, et al. A TILLING reverse genetics tool and a web-accessible collection of mutants of the legume *Lotus japonicus*. *Plant Physiol*. 2003; 131(3):866–71. <https://doi.org/10.1104/pp.102.017384> PMID: 12644638
55. Beveridge CA, Ross JJ, Muref IC. Branching in pea (action of genes *Rms3* and *Rms4*). *Plant Physiol*. 1996; 110(3):859–65. <https://doi.org/10.1104/pp.110.3.859> PMID: 12226224
56. Ishikawa S, Maekawa M, Arite T, Onishi K, Takamura I, Kyozuka J. Suppression of tiller bud activity in tillering dwarf mutants of rice. *Plant Cell Physiol*. 2005; 46(1):79–86. <https://doi.org/10.1093/pcp/pci022> PMID: 15659436
57. Ruyter-Spira C, Kohlen W, Charnikhova T, van Zeijl A, van Bezouwen L, de Ruijter N, et al. Physiological effects of the synthetic strigolactone analog GR24 on root system architecture in Arabidopsis: another belowground role for strigolactones? *Plant Physiol*. 2011; 155(2):721–34. <https://doi.org/10.1104/pp.110.166645> PMID: 21119044
58. Jiang L, Matthys C, Marquez-Garcia B, De Cuyper C, Smet L, De Keyser A, et al. Strigolactones spatially influence lateral root development through the cytokinin signaling network. *J Exp Bot*. 2016; 67(1):379–89. <https://doi.org/10.1093/jxb/erv478> PMID: 26519957
59. De Cuyper C, Fromentin J, Yocgo RE, De Keyser A, Guillotin B, Kunert K, et al. From lateral root density to nodule number, the strigolactone analogue GR24 shapes the root architecture of *Medicago truncatula*. *J Exp Bot*. 2015; 66(1):137–46. <https://doi.org/10.1093/jxb/eru404> PMID: 25371499
60. Halouzka R, Tarkowski P, Zwanenburg B, Cavar Zeljkovic S. Stability of strigolactone analog GR24 toward nucleophiles. *Pest Manag Sci*. 2018; 74(4):896–904. <https://doi.org/10.1002/ps.4782> PMID: 29095562
61. Mayzlish-Gati E, LekKala SP, Resnick N, Winger S, Bhattacharya C, Lemcoff JH, et al. Strigolactones are positive regulators of light-harvesting genes in tomato. *J Exp Bot*. 2010; 61(11):3129–36. <https://doi.org/10.1093/jxb/erq138> PMID: 20501744
62. Mashiguchi K, Sasaki E, Shimada Y, Nagae M, Ueno K, Nakano T, et al. Feedback-regulation of strigolactone biosynthetic genes and strigolactone-regulated genes in Arabidopsis. *Biosci Biotechnol Biochem*. 2009; 73(11):2460–5. <https://doi.org/10.1271/bbb.90443> PMID: 19897913
63. Wong MML, Vaillancourt RE, Freeman JS, Hudson CJ, Bakker FT, Cannon CH, et al. Novel insights into karyotype evolution and whole genome duplications in legumes. *BioRxiv* 099044; 2017.
64. Zhao L, Zhou XE, Wu Z, Yi W, Xu Y, Li S, et al. Crystal structures of two phytohormone signal-transducing α/β hydrolases: karrikin-signaling KAI2 and strigolactone-signaling DWARF14. *Cell research*. 2013; 23(3):436–9. Epub 2013/02/05. <https://doi.org/10.1038/cr.2013.19> PMID: 23381136

65. Xu Y, Miyakawa T, Nakamura H, Nakamura A, Imamura Y, Asami T, et al. Structural basis of unique ligand specificity of KAI2-like protein from parasitic weed *Striga hermonthica*. *Scientific reports*. 2016; 6:31386–. <https://doi.org/10.1038/srep31386> PMID: 27507097
66. Carbonnel S, Das D, Varshney K, Kolodziej MC, Villaécija-Aguilar JA, Gutjahr C. The karrikin signaling regulator SMAX1 controls *Lotus japonicus* root and root hair development by suppressing ethylene biosynthesis. *Proc Natl Acad Sci USA*. 2020;117(35):21757–21765. <https://doi.org/10.1073/pnas.2006111117> PMID: 32817510
67. Mayzlish-Gati E, De-Cuyper C, Goormachtig S, Beeckman T, Vuylsteke M, Brewer PB, et al. Strigolactones are involved in root response to low phosphate conditions in *Arabidopsis*. *Plant Physiol*. 2012; 160(3):1329–41. <https://doi.org/10.1104/pp.112.202358> PMID: 22968830
68. Madmon O, Mazuz M, Kumari P, Dam A, Ion A, Mayzlish-Gati E, et al. Expression of *MAX2* under *SCARECROW* promoter enhances the strigolactone/*MAX2* dependent response of *Arabidopsis* roots to low-phosphate conditions. *Planta*. 2016; 243(6):1419–27. Epub 2016/02/28. <https://doi.org/10.1007/s00425-016-2477-7> PMID: 26919985
69. Sun X, Ni M. HYPOSENSITIVE TO LIGHT, an alpha/beta fold protein, acts downstream of ELONGATED HYPOCOTYL 5 to regulate seedling de-etiolation. *Mol Plant*. 2011; 4(1):116–26. <https://doi.org/10.1093/mp/ssp055> PMID: 20864454
70. Urbański DF, Małolepszy A, Stougaard J, Andersen SU. Genome-wide *LORE1* retrotransposon mutagenesis and high-throughput insertion detection in *Lotus japonicus*. *Plant J*. 2012; 69(4):731–41. <https://doi.org/10.1111/j.1365-3113.2011.04827.x> PMID: 22014280
71. Pimprikar P, Carbonnel S, Paries M, Katzer K, Klingl V, Bohmer MJ, et al. A CCaMK-CYCLOPS-DELLA complex activates transcription of *RAM1* to regulate arbuscule branching. *Curr Biol*. 2016; 26(8):987–98. <https://doi.org/10.1016/j.cub.2016.01.069> PMID: 27020747
72. Kumar S, Stecher G, Li M, Knyaz C, Tamura K. MEGA X: Molecular Evolutionary Genetics Analysis across computing platforms. *Mol Biol Evol*. 2018; 35(6):1547–9. Epub 2018/05/04. <https://doi.org/10.1093/molbev/msy096> PMID: 29722887
73. Trifinopoulos J, Nguyen L, von Haeseler A, Minh BQ. W-IQ-TREE: a fast online phylogenetic tool for maximum likelihood analysis. *Nucleic Acids Research*. 2016; 44(W1):W232–W5. <https://doi.org/10.1093/nar/gkw256> PMID: 27084950
74. Singh S, Katzer K, Lambert J, Cerri M, Parniske M. CYCLOPS, a DNA-binding transcriptional activator, orchestrates symbiotic root nodule development. *Cell Host & Microbe*. 2014; 15(2):139–52. <https://doi.org/10.1016/j.chom.2014.01.011> PMID: 24528861
75. Bayle V, Nussaume L, Bhat RA. Combination of novel green fluorescent protein mutant TSapphire and DsRed variant mOrange to set up a versatile in planta FRET-FLIM assay. *Plant Physiol*. 2008; 148(1):51–60. <https://doi.org/10.1104/pp.108.117358> PMID: 18621983
76. Binder A, Lambert J, Morbitzer R, Popp C, Ott T, Lahaye T, et al. A modular plasmid assembly kit for multigene expression, gene silencing and silencing rescue in plants. *PLoS One*. 2014; 9(2):1–14. <https://doi.org/10.1371/journal.pone.0088218> PMID: 24551083
77. Matsuo K, Shindo M. Efficient synthesis of karrikinolide via Cu(II)-catalyzed lactonization. *Tetrahedron*. 2011; 67(5):971–5. <https://doi.org/10.1016/j.tet.2010.11.108>
78. Irizarry RA, Hobbs B, Collin F, Beazer-Barclay YD, Antonellis KJ, Scherf U, et al. Exploration, normalization, and summaries of high density oligonucleotides array probe level data. *Biostatistics*. 2003; 4(2):249–64. <https://doi.org/10.1093/biostatistics/4.2.249> PMID: 12925520
79. Gentleman RC, Carey VJ, Bates DM, Bolstad B, Dettling M, Dudoit S, et al. Bioconductor: open software development for computational biology and bioinformatics. *Genome Biol*. 2004; 5(10):R80–R. Epub 2004/09/15. <https://doi.org/10.1186/gb-2004-5-10-r80> PMID: 15461798
80. Gautier L, Cope L, Bolstad BM, Irizarry RA. affy—analysis of Affymetrix GeneChip data at the probe level. *Bioinfo*. 2004; 20(3):307–15. <https://doi.org/10.1093/bioinformatics/btg405> PMID: 14960456
81. Smyth GK. limma: Linear Models for Microarray Data. In: Gentleman RC, Carey VJ, Huber W, Irizarry RA, Dudoit S, editors. *Bioinformatics and computational biology solutions using R and Bioconductor*. New York, NY: Springer New York; 2005. p. 397–420.
82. Smyth GK. Linear models and empirical bayes methods for assessing differential expression in microarray experiments. *Statist Appl Genet Mol Biol*. 2004; 3(1):1–26. Epub 2006/05/02. <https://doi.org/10.2202/1544-6115.1027> PMID: 16646809
83. Czechowski T, Bari RP, Stitt M, Scheible W, Udvardi MK. Real-time RT-PCR profiling of over 1400 *Arabidopsis* transcription factors: unprecedented sensitivity reveals novel root- and shoot-specific genes. *Plant J*. 2004; 38(2):366–79. <https://doi.org/10.1111/j.1365-3113.2004.02051.x> PMID: 15078338